frontiers in Marine Science

ORIGINAL RESEARCH
published: 08 November 2018
doi: 10.3389/fmars.2018.00413

Solute Reservoirs Reflect Variability of Early Diagenetic Processes in Temperate Brackish Surface Sediments

Marko Lipka[1], Jana Woelfel[2], Mayya Gogina[3], Jens Kallmeyer[4], Bo Liu[1†], Claudia Morys[5], Stefan Forster[6] and Michael E. Böttcher[1]**

[1] Geochemistry and Stable Isotope Biogeochemistry Group, Marine Geology, Leibniz Institute for Baltic Sea Research (LG), Warnemünde, Germany, [2] Trace Gas Biogeochemistry, Marine Chemistry, Leibniz Institute for Baltic Sea Research (LG), Warnemünde, Germany, [3] Benthology, Biological Oceanography, Leibniz Institute for Baltic Sea Research (LG), Warnemünde, Germany, [4] Section 5.3 Geomicrobiology, Helmholtz Center Potsdam German Geophysical Research Center (GFZ), Helmholtz Association of German Research Centers (HZ), Potsdam, Germany, [5] Estuarine and Delta Systems, Royal Netherlands Institute for Sea Research (NIOZ), Den Burg, Netherlands, [6] Institute for Biosciences - Marine Biology, University of Rostock, Rostock, Germany

Coastal marine sediments are a hotspot of organic matter degradation. Mineralization products of early diagenetic processes accumulate in the pore waters of the sediment, are subject of biological uptake and secondary biogeochemical processes and are released back into the water column via advective and diffusive fluxes across the sediment-water interface. Seven representative sites in the shallow coastal area of the southern Baltic Sea (15–45 m water depth), ranging from permeable sands to fine grained muds, were investigated on a seasonal basis for their key mineralization processes as well as their solid phase and pore water composition to identify the drivers for the variability of early diagenetic processes in the different sediment types. The sandy sediments showed about one order of magnitude lower organic carbon contents compared to the muds, while oxygen uptake rates were similar in both sediment types. Significantly higher oxygen uptake rates were determined in two near-shore muddy sites than in a deeper coastal muddy basin, which is due to higher nutrient loads and the corresponding addition of fresh algal organic matter in the near-shore sites. Pore water concentration profiles in the studied sediments were usually characterized by a typical biogeochemical zonation with oxic, suboxic, and sulfidic zones. An up to 15 cm thick suboxic zone was sustained by downward transport of oxidized material in which dissolved iron and phosphate indicate an intensive reduction of reactive Fe with the release of adsorbed phosphorus. While the geochemical zonation was stable over time in the muds of the studied deeper basin, high variability was observed in the muds of a near-coastal bay probably mainly controlled by sediment mixing activities. The sediments can be characterized by essentially two factors based on their near-surface benthic solute reservoirs: (1) their organic matter mineralization and solute accumulation efficiency and (2) their redox-state. Benthic solute reservoirs in the pore waters of the top decimeter were generally higher in the muddy than in the sandy sediments as the

OPEN ACCESS

Edited by:
Elinor Andrén,
Södertörn University, Sweden

Reviewed by:
Boris Chubarenko,
P.P. Shirshov Institute of Oceanology (RAS), Russia
Björn Grüneberg,
Brandenburg University of Technology Cottbus-Senftenberg, Germany

***Correspondence:**
Marko Lipka
marko.lipka@posteo.de
Michael E. Böttcher
michael.boettcher@io-warnemuende.de

†Present Address:
Bo Liu,
Section Marine Geochemistry, Alfred Wegener Institute Helmholtz Center for Polar and Marine Research, Bremerhaven, Germany

Specialty section:
This article was submitted to Coastal Ocean Processes, a section of the journal Frontiers in Marine Science

Received: *30 April 2018*
Accepted: *17 October 2018*
Published: *08 November 2018*

Citation:
Lipka M, Woelfel J, Gogina M, Kallmeyer J, Liu B, Morys C, Forster S and Böttcher ME (2018) Solute Reservoirs Reflect Variability of Early Diagenetic Processes in Temperate Brackish Surface Sediments. Front. Mar. Sci. 5:413. doi: 10.3389/fmars.2018.00413

more permeable sands were prone to an intensive exchange between pore water and bottom water. The three studied muddy sites showed great dissimilarities with respect to their predominating redox-sensitive metabolites (dissolved iron, manganese, and sulfide). Surface-near advective transport like irrigation of permeable sands and rearrangement of cohesive muds had a particularly strong influence on early diagenetic processes in the studied sediments and were probably the most important cause for the spatiotemporal variability of their benthic solute reservoirs.

Keywords: Baltic Sea, pore water, benthic solute reservoirs, nutrients, sediment mixing, surface sediment, advective transport, early diagenesis

1. INTRODUCTION

Coastal seas constitute only about 1.7 % of the oceans surface area but provide around 18 % of total oceanic net primary production (Field, 1998). The seabeds serve as the main locations of modification and accumulation of particulate matter incorporated into the sediments on deposition (Rullkötter, 2006). Coastal sediments are inherently highly dynamic systems; they display highest sedimentation rates, are affected by waves or near-shore currents and beyond that continuously exposed to human interventions (Talley et al., 2011).

Mineralization of organic material is carried out by microorganisms using oxygen, nitrate, manganese/iron (oxyhydr)oxides, or sulfate as terminal electron acceptors (Froelich et al., 1979). Thermodynamically, oxygen is the most favorable terminal electron acceptor for microbial degradation of organic matter. Due to transport limitations and low saturation concentration of oxygen in sea water, its availability in marine sediments is often limited to the top millimeters to centimeters depending on sediment permeability, irrigation and bioturbation activity (Revsbech et al., 1980; Glud, 2008). Below the thin oxic zone, anaerobic bacteria use alternative electron acceptors to decompose organic matter. Sulfate reduction is the most important anaerobic degradation process in reduced marine sediments (Jørgensen, 1982; Howarth, 1984; Isaksen and Jørgensen, 1996). Highest sulfate reduction activities were observed in estuarine and shallow sea ecosystems, accounting for 20–40 % of the global sulfate reduction (Skyring, 1987). Microbial sulfate reduction is reported to contribute to the organic matter mineralization in continental shelf sediments by more than 50 % (Jørgensen, 1982; Canfield et al., 1993; Wang and Van Cappellen, 1996; Bowles et al., 2014).

Post-depositional processes, including the consumption of terminal electron acceptors, the release of mineralization products (dissolved inorganic carbon, nitrogen, and phosphorus) into the sedimentary interstitial waters, as well as subsequent reactions of produced metabolites (hydrogen sulfide, dissolved iron, and manganese) are reflected by the chemical composition of the solid phase and associated pore waters. Since marine organic matter is mainly composed of carbon, nitrogen, and phosphorus, its mineralization releases dissolved inorganic carbon, nitrogen, and phosphorus into the sediment pore waters. The dissolved substances in the pore water migrate upward and downward along concentration gradients via diffusion and other transport mechanisms. Non-diffusive transport processes like burrowing animals (bioturbation and bioirrigation), hydro-irrigation or anthropogenic influences (bottom trawling or ship anchors) effectively relocate particles and pore water in the surface sediments (Eggleton and Thomas, 2004; Kristensen et al., 2012). These processes, collectively referred to as "advective processes" in this study, transport organic matter and reactive metals into and pore water solutes out of the sediments (Huettel et al., 1996; Huettel and Rusch, 2000; Rusch and Huettel, 2000).

The pore water chemistry of marine sediments is largely influenced by the presence of iron and manganese minerals, which are widely distributed in the environment and common in marine sediments. These minerals are introduced into the marine system via rivers and over the air and play a major role as electron shuttle in suboxic processes, especially iron with its diverse binding forms in different oxidation states (Haese, 2006). Iron and manganese naturally occur in two oxidation states, reduced Mn(II) and Fe(II) (ferrous iron) and oxidized Mn(III/IV) and Fe(III) (ferric iron). Ferric iron phases are highly reactive toward sulfide. Sedimentary iron may also be associated with clay minerals, however, these iron phases are less reactive to microbial activity or reactivity toward hydrogen sulfide than iron (oxyhydr)oxides (Poulton et al., 2004). Also some sulfate reducing bacteria are known to contribute to Fe-reduction in coastal marine sediments (Lovley et al., 1993; Reyes et al., 2016). Thus, in reactive iron-rich layers (suboxic zone) dissolved sulfide is hardly present in pore waters although sulfate reduction occurs; instead dissolved iron accumulates in the suboxic zone (Canfield, 1989; van de Velde and Meysman, 2016). Therefore, the occurrence of dissolved Fe^{2+} in the pore waters marks the suboxic zone, which forms a buffer between the often very thin oxic and the sulfidic zone. This zone has ecosystematic relevance for benthic flora and fauna, which do not tolerate hydrogen sulfide (Wang and Chapman, 1999). Buried Mn-oxides can be reduced by Fe^{2+}, liberating Mn^{2+} into the interstitial waters (Postma and Appelo, 2000) and also ammonia oxidation by Mn-oxides was suggested (Hyacinthe et al., 2001). Mn^{2+} and Fe^{2+} in return can be reoxidized on contact with nitrate or oxygen. Schippers and Jørgensen (2001) discovered a mechanism of anoxic pyrite oxidation by MnO_2 via an Fe(II)/Fe(III)-shuttle, so that no direct contact between the two solid phases is required. Via this redox cascade, most of the produced sulfide is reoxidized by oxidizing agents like iron (oxyhydr)oxides, manganese oxides, nitrate, and finally oxygen (Aller and Rude, 1988; Canfield et al., 1993; Schippers and Jørgensen, 2002).

Consequently, the geochemical composition of the pore waters is determined by microbial organic matter mineralization, transport processes at the sediment-water interface and secondary reactions within the surface sediments. Multi-element pore water solute analysis allows for a detailed biogeochemical characterization of the studied sediments. Pore water concentration profiles are usually used to calculate diffusive solute fluxes across the sediment-water interface or to identify zones of biogeochemical transformations and estimate the transformation rates in the sediment. The accuracy of the result of such estimates highly depends on the depth resolution of the surveyed pore water concentration profiles, which is often limited due to methodological constraints. The conclusions that can be drawn from such calculations are correspondingly confined. In this study we derive a different parameter from pore water concentration profiles, the benthic solute reservoir. To our knowledge, a quantification of the benthic solute reservoirs, i.e. the accumulated amount of dissolved substances in the upper centimeters of the sediment, has not yet been used to characterize sediments regarding their early diagenetic processes. Near-surface benthic solute reservoirs are sum parameters for the characterization of porous sediments concerning biogeochemical reactions and transport processes. Unlike diffuse fluxes or transformation rates, the calculation of benthic solute reservoirs is robust even with lower sampling resolution and less dependent on the pore water concentration profile shape at the dynamic sediment-water interface , i.e., due to short-term changes in bottom waters. Instead, the multi-element benthic solute reservoirs directly reflect mineralization activity, subsequent biogeochemical reactions and transport processes in the considered depth interval.

This study aims to quantify the variability of solute reservoirs in the surface sediments of different sediment types of the southern Baltic Sea and to identify the reasons for the variability in the different early diagenetic processes in surface sediments, including organic matter mineralization, secondary biogeochemical reactions and transport processes.

Previous biogeochemical studies in the Baltic Sea have mostly concentrated on the deep anoxic basins, Gdansk Bay, and the Gulf of Finland. However, the southern Baltic Sea offers a gradient system, that allows to compare muds and sands under different salinity regimes and, as a consequence, differing benthic fauna. In addition to spatial variability, there are also great temporal dynamics in temperature, salinity, and oxygen availability in this shallow coastal area. Most studies on benthic ecosystem services lack such seasonal aspects. The Baltic Sea is also under great pressure from anthropogenic activity (e.g., nutrient input via rivers, shipping traffic). Potential environmental controlling factors responsible for spatial variability or temporal dynamics in the benthic solute reservoirs of the studied coastal surface sediments are discussed.

2. METHODS

2.1. Study Area

The study area is situated in the southern Baltic Sea region (**Figure 1**). This coastal region is characterized by shallow water depths (<50 m), diverse sediment conditions (grain size distribution and organic matter content) and a strong salinity gradient from west (~20) to east (~8). There are two recent sediment accumulation areas, the *Bay of Mecklenburg* and the *Arkona Basin*, with maximum water depths of 26 and 49 m, respectively. In the accumulation areas, about 90 % of the sediment dry weight are clastic components, organic matter makes up ~10 % of the dry weight (Leipe et al., 2011). The occurrence of sandy sediments in the southern Baltic Sea is concentrated along the coasts and in larger areas between the *Bay of Mecklenburg* and the *Arkona Basin* as well as on the *Oder Bank*, a wide flat east of Rügen island (**Figure 1**). The sandy sites are characterized by fine and medium sands (125–500 μm) and low organic carbon contents (<1 % of the dry weight; Leipe et al., 2011).

Seven study sites in the German Baltic Sea region were intensively studied (**Figure 1** and **Table 1**) on a seasonal basis during ten ship-based expeditions between July 2013 and March 2016 (R/V Alkor: 2014-03; R/V Elisabeth Mann Borgese: 2014-06, 2015-01, 2015-04, 2015-08, and 2016-03; R/V Poseidon: 2014-09; R/V Maria S. Merian: 2016-01; see **Supplementary Material** for a detailed list of cruise expeditions). The sites are representative of the major depositional environments. Major events of the year, namely spring- and autumn algal blooms, stagnation periods with bottom water hypoxia and winter dormancy were covered. Two sites within the *Bay of Mecklenburg* were sampled, M-M1 in the inner bay and M-M2 in the outer bay.

The sampling site M-A was situated in the deepest part of the basin inside the exclusion zone for shipping around a monitoring station (**Figure 1**).

Sandy sediments were investigated at two near-coastal sites (S-S and S-D) between the main accumulation areas and on the *Oder Bank* (S-O), a non-depositional sand flat northwest of the *Oder River* mouth (**Figure 1**). The *Oder Bank* sediments are very organic-poor, occasionally overlain by thin fluff (Emeis et al., 1998). A strong variability in sediment type and benthic communities is reported by Laima et al. (1999) for the *Oder Bank*.

An intermediate sediment type with low permeability (comparable to mud) and low organic matter contents (similar to the studied sandy substrates) was studied at the silty I-T site, situated in a shallow bay at the shoulder of northern Rügen. This site is affected by sediment rearrangement during storms (Laima et al., 2001).

2.2. Sediment Sampling

Up to eight parallel short sediment cores were collected with a multicorer in acrylic tubes of 60 cm length and 10 cm internal diameter. Special care was taken to discard sediment cores potentially disturbed during sample collection indicated by e.g., a lower lying or inclined sediment water interface and missing characteristic structures like ripples or macrozoobenthos induced structures in the surface sediments compared to the parallel cores.

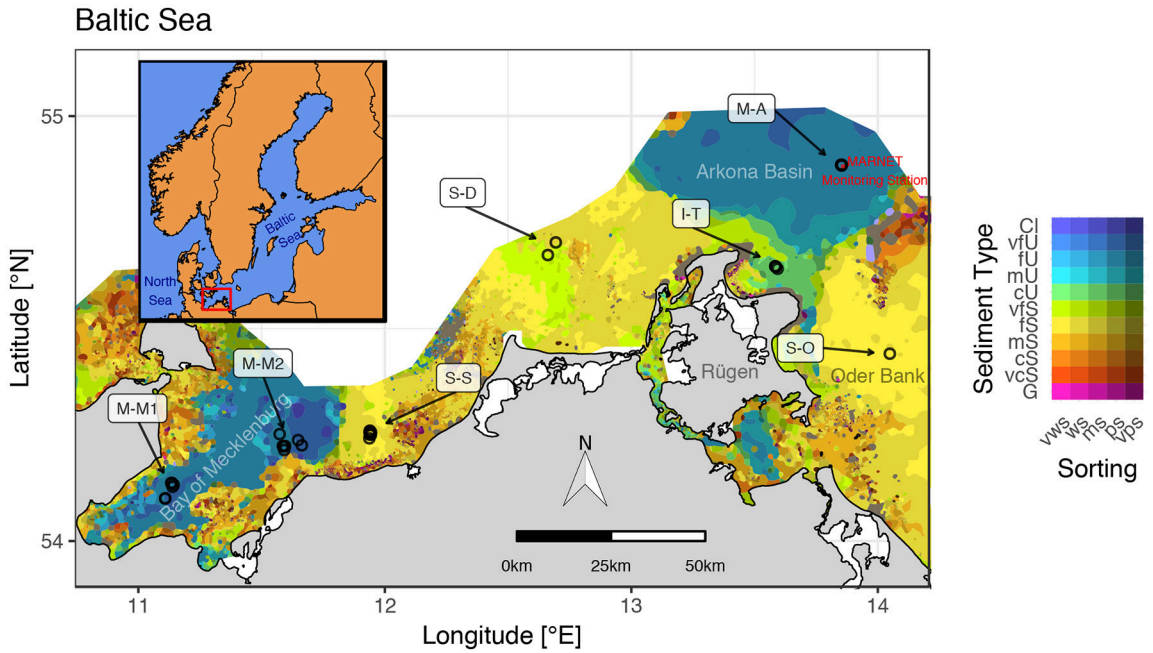

FIGURE 1 | Sampled sites and sediment type distribution in the southern Baltic Sea. Sediment distribution map is redrawn from Tauber (2014). Abbreviations in the legend follow the Wentworth classes: Cl, clay; U, silt; S, sand; G, gravel with graduations of very fine (vf), fine (f), medium (m), and coarse (c). Sediment sorting classes range from very well sorted (vws) over moderately sorted (ms) to very poorly sorted (vps). The red area in the *Arkona Basin* marks the 500 m exclusion zone around a BSH MARNET monitoring station.

TABLE 1 | Sampling sites, their sediment types and typical bottom water temperature, salinity and oxygen concentration investigated in the present study.

Site	Type	Lat. [°N]	Long. [°E]	Depth [m]	T [°C]	Sal	Oxygen [mL/L]
M-M1	Mud	54.1193	11.1336	24	4–14	18–23	1–7
M-M2	Mud	54.2284	11.6069	28	4–14	20–24	0–7
S-S	Sand	54.2531	11.9399	19	4–14	16–22	2–8
S-D	Sand	54.6879	12.6774	22	5–15	13–19	3–8
I-T	Silt	54.6448	13.5870	29	4–16	9–10	5–8
M-A	Mud	54.8848	13.8528	48	5–15	13–24	2–6
S-O	Sand	54.4401	14.0568	17	2–18	8–9	5–9

2.3. Sediment Solid Phase Analysis

Sediment surface chlorophyll *a* (ChlA) contents, a proxy for organic carbon export to the sediments, were analyzed in 6–18 parallel cores per site during four cruises in 2014-09, 2015-01, 2015-04, and 2015-08. According to the method described in Morys et al. (2016), sediment samples of the top 5 mm were extracted for chlorophyll with 96 % ethanol and the extracts were analyzed photometrically.

Sediment samples were retrieved from short cores in 1–2 cm slices. The outer 1 cm rim was immediately trimmed off each slice to avoid cross contamination from adjacent horizons. Sediment slices were transferred into plastic tubes and frozen at –20 °C immediately for subsequent laboratory analysis.

For the classification of the study sites into permeable and impermeable sediments, the dry bulk density (DBD) of the sediment samples was estimated from the water content (determined by weight loss upon vacuum freeze-drying) with the empirical relationship suggested by Flemming and Delafontaine (2000). Sediment porosity was calculated from the water content ($m_{wet} - m_{dry}$), the salt corrected sediment dry weight (m_{solid}) based on the methods suggested by Dadey et al. (1992), the DBD and the density of sea water (ρ):

$$\phi = \frac{V_{water}}{V_{total}} = \frac{m_{water}/\rho}{m_{solid}/DBD} = \frac{(m_{wet} - m_{dry}) \cdot DBD}{\rho \cdot m_{solid}}$$

Sediment permeability was directly measured on sub-cores using a falling head permeameter (Schaffer and Collins, 1966). Hydraulic conductivity, K, was derived from seven to ten consecutive readings of the falling head vs. time, averaged for each measurement (standard deviation ±3–20 % of the mean). Permeability (k) was calculated from hydraulic conductivity

measurements (K) with the following equation:

$$k = \frac{K \cdot \mu}{\rho \cdot g}$$

where μ is the dynamic viscosity, ρ density of sea water, and g the gravitational acceleration.

For a general characterization of the biogeochemical composition of sediments, freeze-dried sediment samples were analyzed for total carbon (TC), total nitrogen (TN), and total sulfur (TS) contents with a CHNS-O *Elemental Analyser EuroEA 3052* from *EuroVector*. Combustion was catalyzed by added *divanadium pentoxide*, the resulting gaseous products were chromatographically separated and measured via infrared spectrophotometry.

Total inorganic carbon (TIC) was determined with a *Macro-Elemental Analyser multi EA* (*Analytik Jena*) by transferring inorganic carbon with 40–50 % phosphoric acid into CO_2, which was then measured by infrared spectrophotometry.

Total organic carbon (TOC) contents were calculated from the difference of TIC and TC contents.

Sedimentary C, N, and S contents were corrected for salinity, compiled and provided by Dennis Bunke (available in Bunke et al., 2018).

Reactive iron (Fe^*) contents were analyzed on freeze dried sediment samples, extracted with 0.5 M HCl solution under constant gentle agitation for 1 h (Kostka and Luther, 1994). Filtered extracts (0.45 µm *Minisart* syringe filters) were analyzed either via photometric analysis (Stookey, 1970) or by inductively coupled plasma optical emission spectrometry (ICP-OES) analysis (*iCAP 6300 Duo Thermo Fisher Scientific*).

Precision and detection limits are given in the **Supplementary Material**.

2.4. Oxygen Uptake

Total oxygen uptake (TOU) is a proxy for the total mineralization activity of a sediment and was studied via *ex-situ* sediment core incubations monitoring oxygen concentrations in the overlying bottom waters. Intact short cores were incubated at constant temperature (5 or 10 °C, depending on ambient bottom water temperature) and under dark conditions for 5–10 d. The bottom water was slowly stirred via magnetic stirrers driven by a rotating magnet outside the core.

Bottom water oxygen concentrations were monitored in high resolution (sampling rate of < 60 s) using in-core attached optode spots with a FIBOX oxygen sensor spot system (*Presens*, Regensburg, Germany). Two-point sensor calibration was performed with aerated sea water (100 % atmospheric saturation) and sea water mixed with sodium dithionite (0 % oxygen). Linear oxygen decline ($R^2 > 0.85$, $p < 0.1$) during oxic (> 89 µM O_2) and hypoxic (< 89 µM O_2) incubation phases were used to calculate TOU rates in the respective incubation phases as follows:

$$TOU = -\frac{\Delta c(O_2)}{\Delta t} \cdot h$$

where $\frac{\Delta c(O_2)}{\Delta t}$ is the concentration gradient over time (slopes of linear model fits) and $h = V/A$ is the height of the water column overlying the sediment in the incubated core (with constant surface area of the core $A = 78.5\ cm^2$).

For an assessment of the influence of macrozoobenthos on the investigated processes, species abundance and biomass were determined after the incubation. Sediment cores were carefully washed on board through a 1 mm mesh sieve and the >1 mm fraction was stored in 4 % buffer formalin solution. Macrozoobenthos species were then sorted in the laboratory, identified at the highest possible taxonomic resolution (species level with the exception of genus *Phoronis* and family *Naididae*) following the World register of Marine Species (WoRMS), counted and weighted. Overall 30 taxa were recorded in 41 incubated cores. Species abundance and biomass was standardized to the area of 1 m^2.

2.4.1. Sulfate Reduction Activity

In order to determine the proportion of anaerobic processes in the total mineralization gross sulfate reduction rates (SRR) were analyzed by the ^{35}S radio-tracer injection technique (Jørgensen, 1978) in the laboratories of the German Research Centre for Geosciences (GFZ). Intact sediment short cores for the analysis were sampled during a summer (August 2015) and a winter (January 2016) campaign from sandy (S-S and S-O) and muddy (M-M1, M-M2, and M-A) sites and stored with supernatant water and head space of air at 4 °C until start of the experiments (November 2015 and February 2016). Rates of ^{35}S-sulfide formation were measured by incubation experiments with $^{35}SO_4^{2-}$ radio-labeled sediments after Fossing (1995) and Kallmeyer et al. (2004).

Sediment incubations were performed either in glass tubes (6 cm long and ~1 cm inner diameter, November 2015) or in sub-cores (3.5 cm inner diameter, February 2016). Transfer of sediment sub-samples into glass tubes was carried out in an inert gas (Ar) atmosphere two days before the start of the incubation experiments. Sub-sampling via sub-cores occurred right before the tracer injection with small liners having silicone-filled injection ports arranged vertically at 1 cm intervals down to 15 cm.

Volumes of 15 µL $^{35}SO_4^{2-}$ tracer solution (*Hartmann Analytic GmbH*, Braunschweig, Germany) with a specific activity of 2.6–5.2 kBq μL^{-1} were injected into each glass tube or injection port so that each sediment sub-sample or sub-core interval contained a radiotracer activity of about 39–78 kBq.

Sub-cores or glass tubes were incubated under dark conditions at near *in-situ* temperature (chosen on the basis of field measurements in the bottom water) for 8 h (at 10 °C in November 2015) or 14.5 h (at 4 °C in February 2016). The sediment sub-cores were sliced into 1 cm (upper 5 cm) or 2 cm (5–15 cm) sections after incubation. Sediment slices or contents of incubated glass tubes were immediately mixed with a 20 % ZnAc solution to fix sulfides and inhibit further sulfate reduction activity.

The cold chromium distillation procedure (Kallmeyer et al., 2004) was used to recover radio-labeled sulfide from the sediment. Radioactivity of ^{35}S was determined using a liquid scintillation counter (*Packard 2500 TR*) with a counting window of 4–167 keV.

2.5. Pore Water Sampling

Immediately after recovery of the sediment short cores, pore water samples were extruded from about 1, 2, 3, 4, 5, 7, 9, 11, 15, and 20 cm below as well as from bottom water right above the sediment-water interface through pre-drilled holes using Rhizons (Rhizosphere, Wageningen, The Netherlands; Seeberg-Elverfeldt et al., 2005) attached to clean syringes (Winde et al., 2014). About 10 mL pore water were extracted from each depth after discarding the first 1–2 mL. Additional filtering of the water samples was not necessary, as the Rhizon samplers consist of microporous tubes with a pore width of 0.2 μm. The water samples were transferred into different sample containers for later analysis: Without delay, 2 mL of pore water were fixed with 5 vol.% Zn-acetate solution for later analysis of sulfide concentration. Samples for major and trace element analysis were filled into pre-conditioned (with 2 % nitric acid) 2 mL sample tubes and acidified to 2 vol.% HNO_3 for conservation. Three milliliters Exetainers (pre-cleaned with 2 % nitric acid, subsequently washed with MilliQ water) prepared with 25 μL saturated mercury chloride solution were filled with no head space for later analysis of dissolved inorganic carbon (DIC).

2.6. Water Analysis

Dissolved Na, Si, S, Fe, Mn, and P in the water samples were analyzed with an ICP-OES (*iCAP 6300 Duo Thermo Fisher Scientific*). Water samples were diluted with 2 % HNO_3 to a target salinity of 3, 6, or 12 depending on the salinity of the samples, estimated from bottom water salinity (measured with a ship based CTD system, e.g., *911+*, *Sea-Bird Electronics*, USA). Measurements were validated with the certified seawater reference standards *CASS-5* or *SLEW-3* (*National Research Council of Canada*, Ottawa, Canada). An additional reference standard mixed with spike solution containing P, Fe, and Si was routinely used, since concentrations of these elements can be distinctly higher in pore water samples than in the reference material (Kowalski et al., 2013).

Dissolved ammonium (NH_4^+) concentrations were analyzed shipboard using standard photometric methods (Grasshoff et al., 2009) on a *QuAAtro* multianalyser system (*Seal Analytical*, Southampton, UK) within hours after sampling and checked with a multi-ion standard solution (*Bernd Kraft GmbH*, Duisburg, Germany; Winde et al., 2014).

Dissolved inorganic carbon (DIC) was measured by means of continuous-flow isotope-ratio-monitoring mass spectrometry (CF-irmMS) using a *Thermo Finnigan MAT 253* gas mass spectrometer coupled to a *Thermo Electron Gas Bench II* via a *Thermo Electron Conflo IV* interface. In an aliquot of the water samples, DIC was transferred to gaseous CO_2 by the manual injection of supersaturated phosphoric acid into *Exetainers* in a thermo-constant *Gas Bench*. Solutions were allowed to react for at least 18 h before introduction into the mass spectrometer (Winde et al., 2014). Aqueous $NaHCO_3$ solutions and solid carbonates were used for concentration calibration.

Dissolved sulfide concentrations in pore waters were determined in 5- to 100-fold diluted samples by the methylene blue technique (Cline, 1969) using a *Spekol 1100* spectrophotometer (*Analytik Jena*).

Precision, accuracy and detection limits of the analysis are given in the **Supplementary Material**.

2.7. Calculations and Statistics

Calculations and statistical analysis were conducted using R version 3.4.2 (R Core Team, 2016). Averages are given as mean ± one standard deviation. To test for statistical significance of the difference between means of group samples, *Bartlett's test* was used to check the homogeneity of variances, normality was checked with *Shapiro-Wilk test* on the *ANOVA* residuals. As *ANOVA* assumptions were not met, the *Kruskal–Wallis H test*, a non-parametric alternative to one-way *ANOVA*, and *Dunn's post-hoc test*, was performed. Unless otherwise stated, hypotheses were tested at a 0.05 level of significance.

Benthic solute reservoirs were calculated from the pore water concentration gradients of the respective solutes as the integrated concentration in the top 10 cm. This corresponds to the cumulated substance quantity in this layer. An integration depth of 10 cm was chosen to avoid the exclusion of some short sandy cores from the comparative analysis.

Principal component analysis (PCA) were performed on benthic solute reservoirs (DIC, H_2S, Fe^{2+}, Mn^{2+}, NH_4^+, PO_4, and H_4SiO_4). Data was zero-centered and scaled to unitary variance before the analysis.

3. RESULTS

3.1. Sediment Solid Phase

3.1.1. Porosity and Permeability

Sediment porosity in the southern Baltic Sea sampling sites was >80 % in muddy sites and ~40 % in sandy sites (**Figure 2**). Porosity profiles showed highest values at the sediment-water interface and decreased with depth due to compaction.

The sandy sites S-O and S-S display permeability values (k_i) of $10 \cdot 10^{-12}\ m^2$ and $4.2 \cdot 10^{-12}\ m^2$ respectively, while permeability in the muddy sites M-A, M-M1, and M-M2 was 2–3 orders of magnitude lower ($k_i = 4.5 \cdot 10^{-14}\ m^2$, $8.2 \cdot 10^{-14}\ m^2$, and $3.6 \cdot 10^{-14}\ m^2$, respectively). S-D and I-T were not analyzed for permeability, but they displayed porosity values (**Figure 2**) and grain size distributions (pers. comm. Dennis Bunke, IOW) comparable to the S-O and M-A sediments, respectively. Hence, the sandy sites S-S, S-D, and S-O can be classified as permeable while the muddy and silty sites M-M1, M-M2, M-A, and I-T must be considered impermeable.

3.1.2. Surface Sediment Chlorophyll

Chlorophyll *a* (ChlA) contents in the top 5 mm of the studied sediments, representing input of fresh organic matter to the sediments, ranged between 2 and 17 $\mu g\ cm^{-2}$ during four cruises between 2014-09 and 2015-08 capturing different seasons (**Figure 9**). Surface sediment ChlA contents were overall lowest at the sandy site S-O ($3.8 \pm 1.1\ \mu g\ cm^{-2}$), significantly higher in the M-A muds ($5.1 \pm 1.7\ \mu g\ cm^{-2}$) and S-S sands ($5.5 \pm 2.6\ \mu g\ cm^{-2}$) and highest at the muddy sites M-M1 ($10.3 \pm 3.5\ \mu g\ cm^{-2}$) and M-M2 ($9.4 \pm 3.0\ \mu g\ cm^{-2}$). The silty site I-T was only analyzed once during this study and

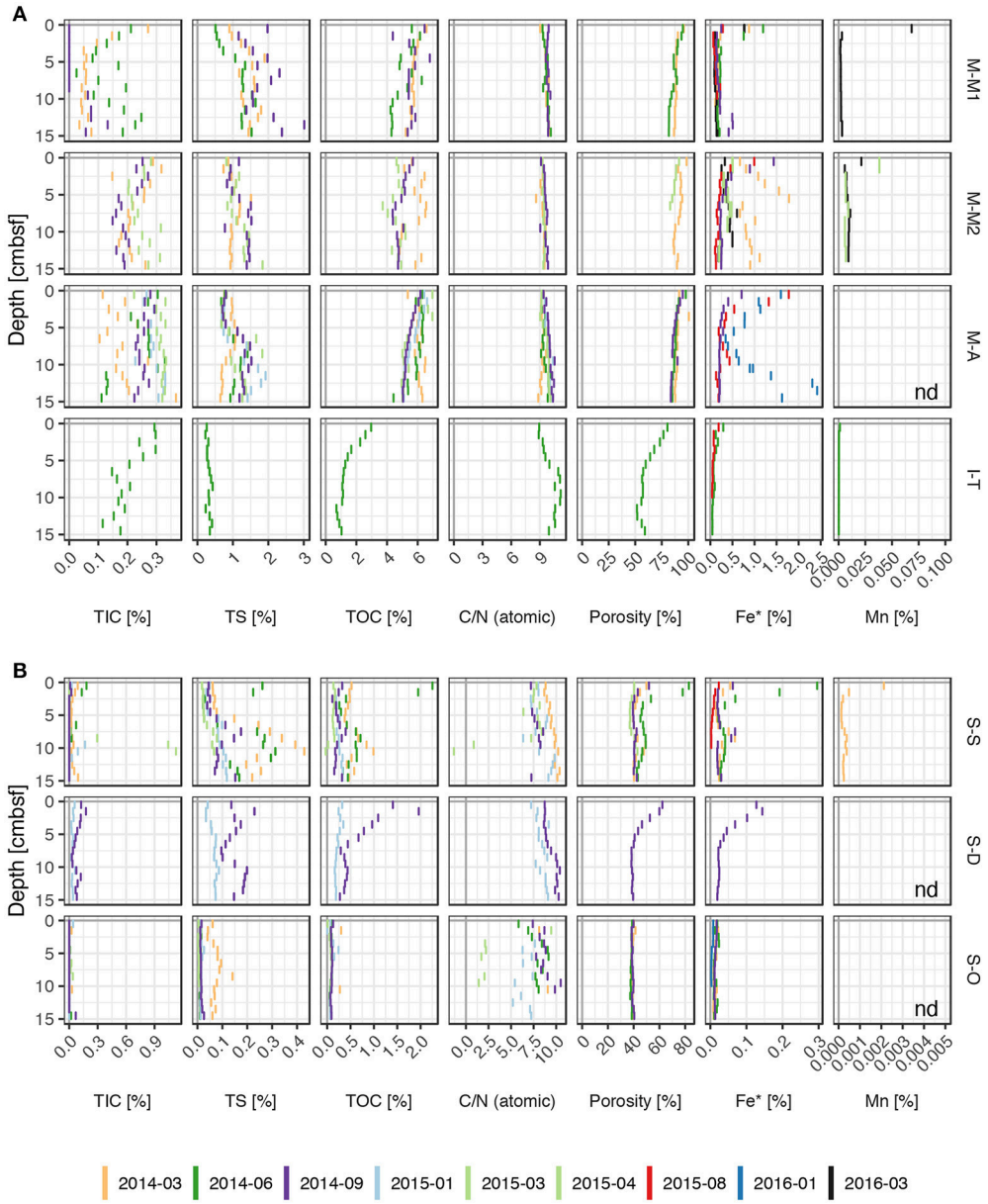

FIGURE 2 | Depth dependent dry mass content of sediment total inorganic carbon (TIC), total organic carbon (TOC), atomic TOC:TN ratio, reactive iron (Fe*), and acid extractable manganese (Mn) in **(A)** silty/muddy and **(B)** sandy sediments. Each bar represents one sediment sample, bar heights indicate the sampling interval. nd, not determined.

showed comparatively high ChlA contents (8.9 ± 0.6 μg cm^{-2}) statistically indistinguishable from the M-M1 and M-M2 muds.

3.1.3. Sediment Solid Phase Composition

Muddy sediments (M-M1, M-M2, and M-A) were statistically indistinguishable in their TIC, TS, and TOC contents of the top 15 cm, indicating a largely homogeneous geochemical composition. However, the muds were characterized by about an order of magnitude higher mean contents of TOC (5.5 ± 0.7 %) compared to the sandy sites (S-S, S-D, and S-O) with TOC contents of 0.3±0.3 % in the top 15 cm (**Figure 2**). The sandy sites occasionally showed surface peaks of more than 2 % (e.g., S-D in September 2014 and S-S in June 2014), indicating temporally or spatially variable input of organic matter. Sedimentary TOC/TN-ratios generally increased with depth, suggesting a preferred degradation of organic nitrogen compounds, thus depletion of N in the more refractory organic matter fraction.

The silty site I-T showed mud-like composition in the top parts of the sediments and a more sand-like composition at depth. Besides, the depth gradients of TOC and the TOC/TN-ratio were large compared to the other sites, indicating a non-steady-state during the single sampling occasion.

Reactive iron and manganese contents of up to approximately 2.5 and 0.07 %, respectively, were measured in the studied muds and about an order of magnitude lower contents were found in the organic-poor sands and silts (**Figure 2**). Fe^{*} and acid extractable Mn usually showed peak contents at the sediment surface exponentially decreasing with depth within the top 2–7 cm. Occasionally, another peak with contents above the background value occurred below. While pyrite does not belong to the still reactive iron fraction (Fe^{*}), as it is not dissolved during acid extraction, amorphous mono-sulfide (FeS) does (Haese, 2006). Fe-sulfides may additionally contribute to the reactive iron fraction due to reoxidation prior to extraction (Böttcher and Lepland, 2000).

3.2. Organic Matter Mineralization

3.2.1. Total Oxygen Uptake

Total oxygen uptake (TOU) is a measure of organic matter mineralization in sediments underlying oxygenated bottom water. The initial TOU rates of the studied sediments in the southern Baltic Sea ranged from 1.5 to 15.5 mmol m^{-2} d^{-1} (**Figure 3**). These rates are at the lower end of previously reported values in coastal muddy and sandy sediments, which vary widely from 4 to ~50 mmol m^{-2} d^{-1} (Jørgensen, 1977; Balzer, 1984; Jørgensen and Revsbech, 1989; Mackin and Swider, 1989; Jensen et al., 1995; Conley et al., 1997; Rysgaard et al., 2001; Janssen et al., 2005; Almroth et al., 2009; Bonaglia et al., 2014).

During summer, bottom water conditions were often already hypoxic or the transition to hypoxic situations occurred during the incubations. Considering only incubation phases with oxic bottom water conditions, average TOU were 5.1 ± 2.2 mmol m^{-2} d^{-1} and 4.9 ± 3.8 mmol m^{-2} d^{-1} in muddy and sandy sites, respectively (statistically not distinguishable). Within the studied muds, TOU in the sites M-M1 and M-M2 of the muddy *Bay of Mecklenburg* were significantly higher (7.3 ± 3.0 mmol m^{-2} d^{-1} and 5.9 ± 1.1 mmol m^{-2} d^{-1}, respectively) than in the muddy site M-A (3.6 ± 0.8 mmol m^{-2} d^{-1}). Oxygen uptake rates of the studied sandy sites S-S and S-O (3.8 ± 1.7 mmol m^{-2} d^{-1} and 5.3 ± 4.7 mmol m^{-2} d^{-1}, respectively) were statistically not distinguishable.

Exceptionally high infauna biomass was responsible for particularly high total oxygen uptake rates in one of the cores in April 2015 (**Figure 4**). The differences within the muds did not correlate with macrozoobenthos abundance or biomass, although very low bioturbation potential of the enclosed macrozoobenthos in the incubation cores of the site M-M1 prevailed. More details on benthic infauna and their influence on the biogeochemistry of the studied sediments can be found in Gogina et al. (in review) (this issue).

3.2.2. Gross Sulfate Reduction

The proportion of sulfate reduction, the most important anaerobic degradation process in reduced marine sediments, was investigated via gross sulfate reduction rate analysis in the studied sediments. The radio-tracer experiments revealed microbial sulfate reduction in all cores, muddy and sandy, with volumetric rates ranging from ~1 to ~100 nmol cm^{-3} d^{-1} (**Figure 5**). Sulfate reduction rates (SRR) of ~100 nmol cm^{-3} d^{-1} are typical for organic-rich, muddy sediments in eutrophic coastal environments, while much lower rates are usually found in continental slope and deep sea sediments (Canfield et al., 2005). The downward decreasing trend of SRR was not due to sulfate limitation but indicates exhaustion of labile organic pools with depth (Boudreau and Westrich, 1984) and a decrease in cell numbers of active sulfate reducing bacteria (Llobet-Brossa et al., 2002; Al-Raei et al., 2009). Sharp local maxima in the top mm below the sediment-water interface followed by a broad sulfate

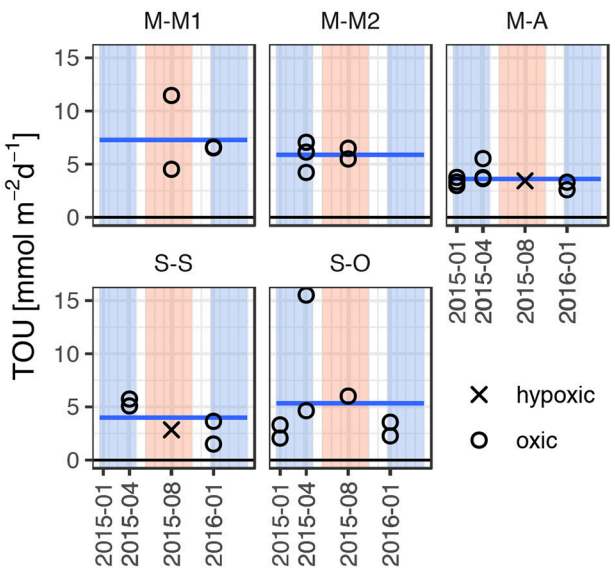

FIGURE 3 | Seasonal record of total oxygen uptake (TOU) rates in southern Baltic Sea sediments obtained via core incubation. Summer (June–October) and winter (January–April) season are highlighted by red and blue shaded areas, respectively. Horizontal blue lines represent the mean total oxygen uptake rate over all incubations for each site.

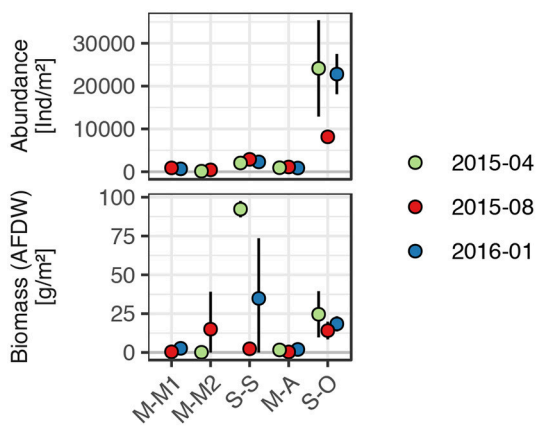

FIGURE 4 | Total macrozoobenthos abundance and biomass (ash free dry weight) in the incubated short cores. Points and errorbars represent means ± one standard deviation of 2 to 4 cores.

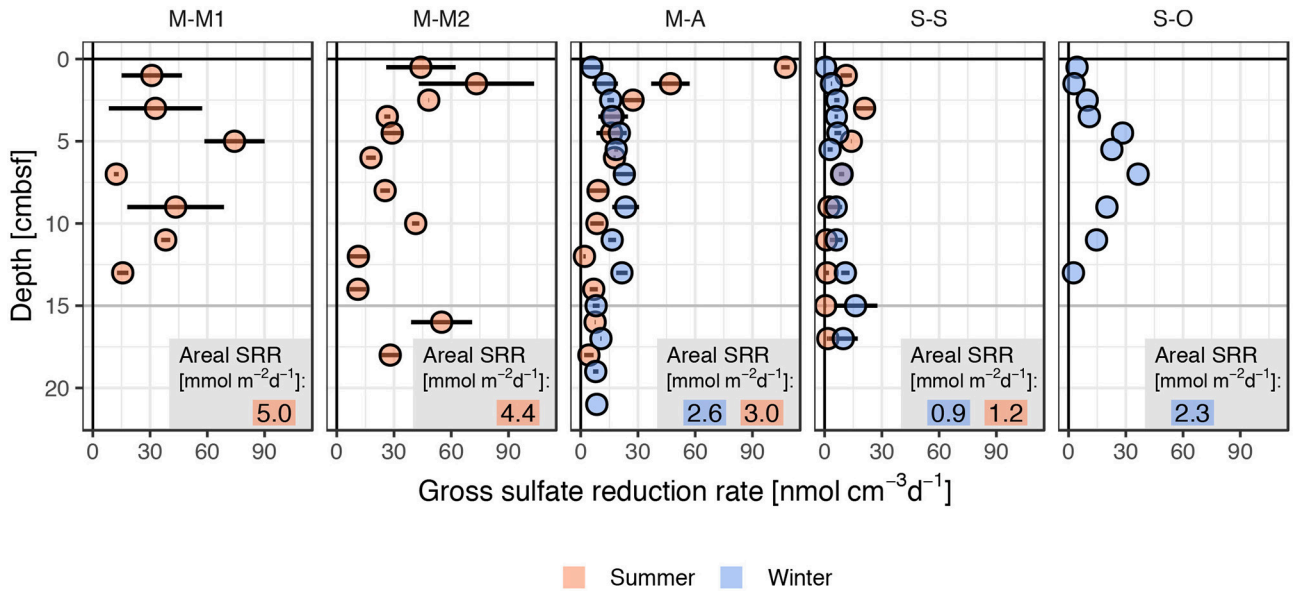

FIGURE 5 | Vertical distribution of sulfate reduction rates measured in muddy (M-A, M-M1, and M-M2) and sandy (S-S and S-O) study sites in summer and winter. Values are given as mean and range of two replicates except for S-O, where only one core was incubated. Areal SRR [*mmol* m^{-2} d^{-1}] are shown separately for summer and winter as depth-integrated sulfate reduction rates in the top 15 cm of the sediments.

reduction zone below are frequently reported in the literature (Moeslund et al., 1994; Kristensen, 2000; Sawicka et al., 2012).

Highest rates (~100 nmol cm^{-3} d^{-1}) at the surface of M-A muddy sediments during summer 2015 may be explained by increased organic matter supply from algal bloom detritus. M-M1 and M-M2 sediments, however, did not show a clear depth dependence in sulfate reduction but overall higher values in depths >5 cm compared to the site M-A.

Overall lowest values were measured in the sandy site S-S.

Depth integrated SRR in the top 15 cm measured during this study ranged from 0.9 to 5.0 mmol m^{-2} d^{-1} (**Figure 5**). These measures are in good agreement with average sulfate reduction rates for non-depositional (1.1 mmol m^{-2} d^{-1}) and depositional (4.7 mmol m^{-2} d^{-1}) shelf sediments compiled by Canfield et al. (2005). Thode-Andersen and Jørgensen (1989) reported integrated sulfate reduction rates (top 15 cm) in fine grained organic-rich coastal sediments (Aarhus Bay, Denmark) of 1.1–3.8 mmol m^{-2} d^{-1}, which matches the measured SRR at site M-A (2.6 and 3.0 mmol m^{-2} d^{-1}) but is distinctly lower than the values observed for the sites M-M1 and M-M2 (4.4 and 5.0 mmol m^{-2} d^{-1}; **Figure 5**). In the central deep basin of the Baltic Sea, the *Gotland Deep* with organic-rich silty sediments and usually anoxic bottom waters, depth integrated SRR (20 cm) of 4.8 mmol m^{-2} d^{-1} (Al-Raei & Böttcher, unpubl. results) and 3.8–7.6 mmol m^{-2} d^{-1} (Piker et al., 1998) were reported. These measures are comparable to southern Baltic Sea SRR found at muddy sites in this study. Considerably higher rates (13.5 mmol m^{-2} d^{-1} in top 20 cm) were observed in the *Landsort Deep* (Al-Raei et al. unpublished). Both sites are located in the deep basins with temporarily anoxic bottom waters and were anoxic at the time of sampling. Hence, sulfate reduction was most likely the dominating mineralization pathway here.

Werner et al. (2006) reported integrated SRR (top 15 cm) of ~2.2 mmol m^{-2} d^{-1} for the Janssand intertidal sand flat (Spiekeroog, North Sea, Germany), which is close to the value observed in the sandy S-O sediments during this study. In contrast, integrated sulfate reduction rates of 1.9–34 mmol m^{-2} d^{-1} were reported for the top 15 cm of temperate intertidal sediments in the German Wadden Sea of the southern North Sea (Böttcher et al., 2000; Kristensen, 2000). Al-Raei et al. (2009) reported seasonally dynamic integrated SRR in North Sea intertidal surface sediments (top 15 cm) ranging from ~6 – 30 mmol m^{-2} d^{-1} (mixed type sediments) to ~1 – 16 mmol m^{-2} d^{-1} (sands). Although obtained from a coastal sea in the same climate zone in sediments with similar TOC contents, these rates are considerably higher than those found in the Baltic Sea sediments during this study. In the compilation of sulfate reduction rates from different marine depositional settings (Canfield et al., 2005), intertidal sediments showed two to tenfold higher values compared to the listed shelf sediments.

3.3. Pore Water Profiles

The pore water concentration profiles (**Figure 6**) were consistent with the typical pore water zonation below mostly oxic bottom waters (Jørgensen and Kasten, 2006). Differences between the profile shapes of parallel cores are usually small compared to the temporal variability of the pore water profiles so that spatial homogeneity can be assumed within the individual sites. Most pronounced in muddy sediments (**Figure 6A**), pore water profiles in the top 20 cm were dominated by intense net sulfate reduction, indicated by decreasing SO_4^{2-} and increasing H_2S concentrations with increasing depth.

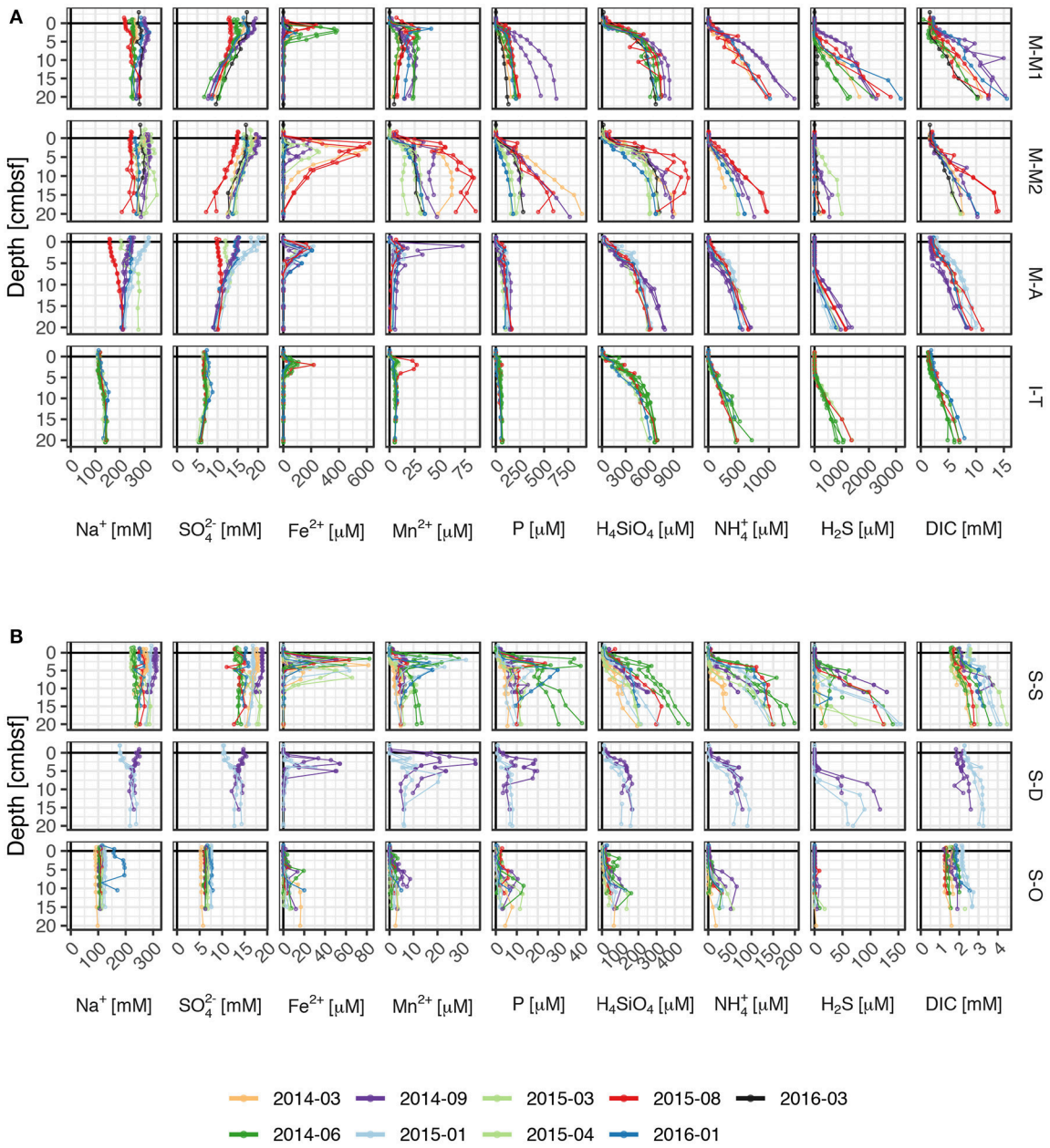

FIGURE 6 | Multi-parameter pore water concentration profiles in **(A)** soft sediments and **(B)** sandy sediments.

Active manganese and iron reduction were indicated by the presence of dissolved manganese (Mn^{2+}) and iron (Fe^{2+}) in the pore waters. The appearance of H_2S consistently coincided with Fe^{2+} depletion at depth. All organic matter mineralization processes released dissolved inorganic carbon (DIC, mainly HCO_3^- at pH 8), ammonium (NH_4^+) and phosphate (mainly as HPO_4^{2-} at pH 8) into the interstitial waters.

Orders of magnitude lower concentrations were found in sandy and organic-poor sediments (**Figure 6B**). No decrease in sulfate with depth and only low concentrations of dissolved sulfide (up to 150 µM) were found at depths >10 cm. Active manganese and iron reduction was indicated by increased Fe^{2+} and Mn^{2+} concentrations and also primary mineralization products (DIC, NH_4^+, H_4SiO_4, and PO_4) accumulated at depth to a lesser extent.

3.4. Benthic Solute Reservoirs

Especially the primary products of organic matter mineralization dissolved inorganic carbon (DIC), dissolved inorganic nitrogen (DIN, mainly NH_4^+), and dissolved inorganic phosphorus (DIP, mainly PO_4), accumulate in surface sediment interstitial waters

(**Figure 6**). Also sulfide (H_2S) concentrations were usually high in pore waters of the muddy sites, as sulfate reduction is an important process in the studied muds (**Figure 5**). Consequently, these solutes showed orders of magnitudes higher concentrations in the pore waters compared to the overlying water column, forming substantial solute reservoirs in the surface sediments (**Figure 7**). Benthic reservoirs of all considered solutes (H_4SiO_4, NH_4^+, PO_4, DIC, sulfide, Fe^{2+}, and Mn^{2+}) in the top 10 cm surface sediment were generally higher in studied muds than in the sandy study sites, while the silty site I-T showed intermediate values (**Figure 7**).

Benthic solute reservoirs were largest in the organic-rich and impermeable muds, smaller in the intermediate silt and close to zero in the sandy sediments (**Figure 7**). DIC formed by far the largest benthic solute reservoirs (about 450 mmol m^{-2} in the muds), followed by H_4SiO_4 and NH_4^+ (about 42 and 25 mmol m^{-2} in the muds; C:Si:N = 106:10:6). This is approximately in line with the Redfield-Brzezinski compositions of marine organic matter or diatoms, assuming that organic matter mineralization products are released into the pore waters with a ratio of C:Si:N:P = 106:15:16:1 (Redfield, 1958; Brzezinski, 1985). Smaller Si and N reservoirs compared to C in the pore waters may be attributed to limited solubility of biogenic silica and ammonium reoxidation via nitrification. Phosphate reservoirs, on the other hand, were on average 15 mmol m^{-2} in the muds (C:Si:N:P = 106:10:6:4). Due to a higher degradability of organic P and N components, these can be preferentially released relative to C during the initial stages of organic matter mineralization. In the long run, however, metabolites are often released in stoichiometric relation of the bulk composition of reactive organic matter (Burdige, 2006). High PO_4 reservoirs relative to DIC indicate the release of adsorbed P from reactive Fe phases rather than through mineralization of organic matter.

The redox-sensitive pore water constituents (sulfide, Fe^{2+}, and Mn^{2+}) only accumulate to considerable reservoirs in the fine-grained sediments.

A Principal Component Analysis (PCA) based on the benthic solute reservoirs (DIC, NH_4^+, PO_4, H_4SiO_4, sulfide, Fe^{2+}, and Mn^{2+}) of the studied sediments revealed that the first two principal components explain 89 % of the observed variance (**Figure 8B**) allowing for a virtually undistorted two-dimensional visualization of the dissimilarity between the study sites at different points in time (**Figure 8A**). Sandy sites clearly cluster on the left and muddy sites on the right hand side of the y-axis, while silt situates between these two clusters (**Figure 8A**). Variability, represented by the size of the spanned areas in **Figure 8A**, was highest in the muds and considerably smaller within the sandy sites. Strikingly, the individual sites are almost completely distinguishable in the PCA plot (**Figure 8A**). The results were practically independent of the chosen sediment depth over which the substance quantities were cumulated to benthic solute reservoirs (tested on values between 5 and 20 cm). Using benthic solute reservoirs of the top 15 cm as a basis for the PCA analysis (instead of 10 cm), the number of available data (especially from sandy sites) is reduced but results are generally very similar (see **Supplementary Material**).

4. DISCUSSION

4.1. Organic Matter Mineralization

Oxygen uptake of 5.0 ± 2.9 mmol m^{-2} d^{-1} and depth integrated (top 15 cm) gross sulfate reduction rates of 0.9–5.0 mmol m^{-2} d^{-1} indicate active organic matter mineralization with substantial contribution of sulfate reduction in the studied muddy and sandy sediments. The study sites differed primarily in their sediment type which is reflected most clearly in their varying permeability and organic matter contents. Organic matter content in sediments can be described as a reactive continuum, where rapid degradation of freshly deposited organic matter takes place near the sediment surface, while a large fraction of deeper buried organic matter is rather refractory (Berner, 1980). Sands have often been treated as generally unreactive sediments due to their lack of TOC and reactive substances. However, recent studies show that substantial mineralization of highly degradable organic matter occurs in sandy sediments while accumulation of aged material and mineralization products is prevented by advective transport processes (Boudreau et al., 2001; Huettel et al., 2014). Huettel and Gust (1992) and Ziebis et al. (1996) demonstrated strong advective pore water flushing down to several centimeters sediment depth caused by boundary layer flows over a rough sea floor. Such bedform-induced interfacial flows also lead to uptake of particulate organic matter into permeable shelf sediments (Huettel et al., 1996; Huettel and Rusch, 2000; Rusch and Huettel, 2000), which is the source of the reactive organic matter for mineralization processes. Occasionally increased TOC contents throughout the top 2–5 cm in the studied sandy sediments indicate such short-term incorporation of organic matter (**Figure 2**, e.g., S-S in 2014-06 or S-D in 2014-09).

Significantly increased TOU rates and SRR were measured in the *Bay of Mecklenburg* (M-M1 and M-M2) compared to the *Arkona Basin* (M-A), although TOC contents of the different muds were statistically indistinguishable (**Figure 2**). However, statistically significant higher ChlA contents were detected at the sediment surface of sites M-M1 and M-M2 (9.5 ± 3.1 μg cm^{-2} and 8.3 ± 3.3 μg cm^{-2}) than at site M-A (4.6 ± 1.7 μg cm^{-2}) during four cruises of this study (**Figure 9A**). There was also significant correlation between the oxygen uptake rates and the ChlA contents in the top 0.5 cm of the studied muds (**Figure 9B**). Consequently, differences in mineralization intensity between the studied muds were rather controlled by spatially varying input of readily degradable organic matter than by the standing TOC stock. This is in accordance with several studies after which the supply of labile organic material from the water column is a main factor controlling mineralization rates in sediments (Middelburg, 1989; Graf, 1992; Middelburg et al., 1993; Arndt et al., 2013).

4.2. Benthic Solute Reservoirs in Different Sediment Types

The PCA analysis of the benthic solute reservoirs revealed that the variability between the studied sediments can be expressed by

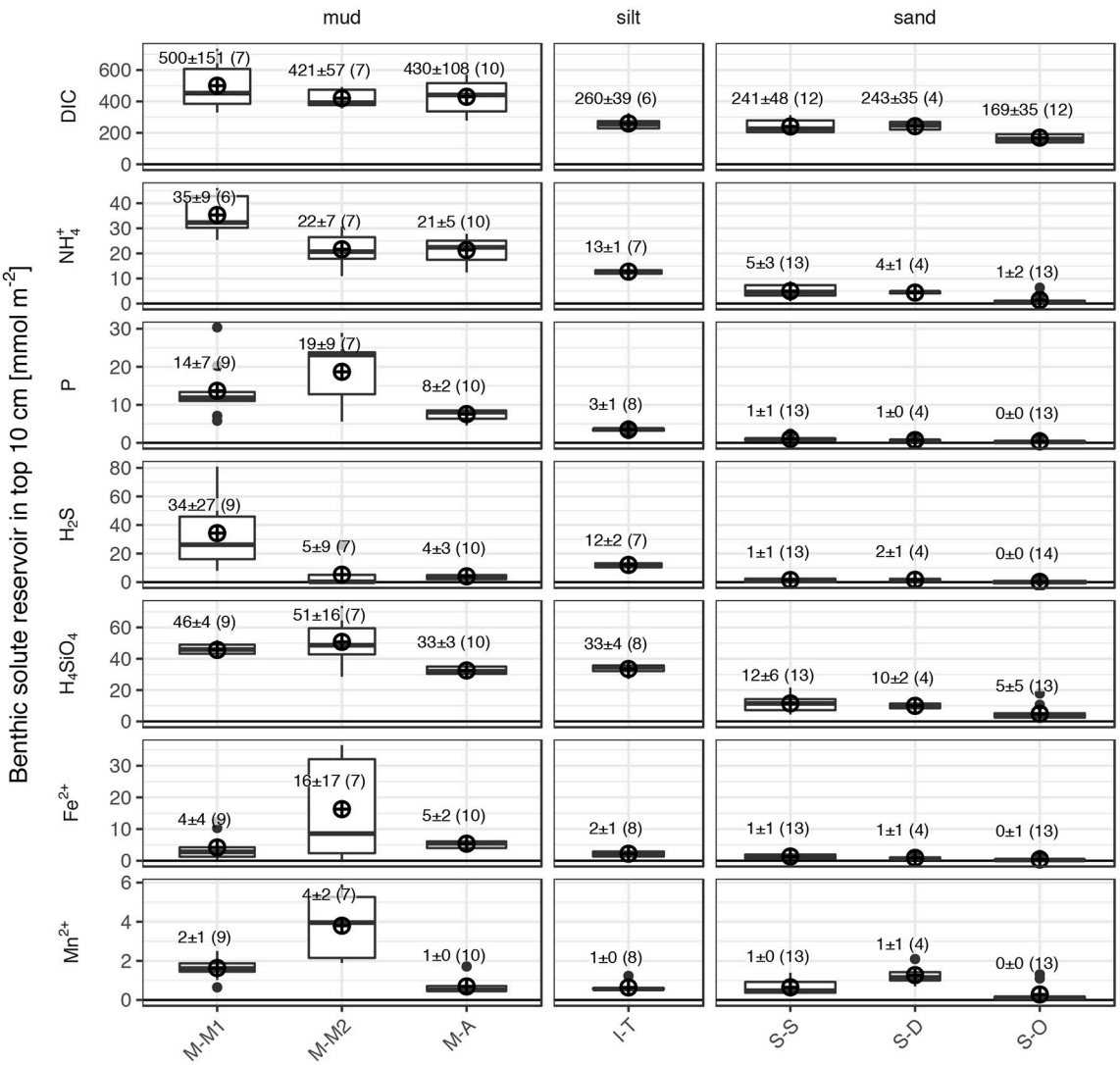

FIGURE 7 | Benthic solute reservoirs of the top 10 cm of the southern Baltic Sea sediments calculated from the pore water profiles shown in **Figure 6** and visualized by boxplots. Each boxplot summarizes the data from multiple pore water profiles for each site and parameter. The lower and upper hinges of the boxes correspond to the 25 and 75th percentiles, the line within the boxes represents the median. The whiskers extend from the hinges to the largest and smallest value inside the 1.5-fold inter-quartile range. Labeled ⊕ mark the arithmetic mean reservoir size of each subset (± one standard deviation, number of cores in brackets).

essentially two principal components. The principal component *PC1* alone explained 68 % of the variability (**Figure 8B**). All considered parameters substantially contributed to this component but the primary organic matter mineralization products DIC, NH_4^+, PO_4, and H_4SiO_4 dominate (**Figure 8C**). As similar rates of organic matter mineralization were observed in sand and mud, similar amounts of mineralization products must be released into the pore waters. The significantly smaller reservoirs in the studied sands therefore indicate the removal of mineralization products from the pore space back into the water column via advective transport processes. *PC1* can therefore be regarded as a factor representing the degree of organic matter mineralization and subsequent release of dissolved substances into the pore waters and the potential of the sediment to accumulate these solutes in form of benthic reservoirs. This mineralization and solute accumulation efficiency factor was above average in low-permeable and organic-rich muds and below average in the sands (**Figure 8A**).

Although substantial gross sulfate reduction (**Figure 5**) and oxygen uptake (**Figure 3**) rates were observed at site S-O, these sands showed the lowest benthic solute reservoirs of all studied sites (**Figure 7**), significantly lower than the other studied sands. Thus, the S-O sands were least accumulative for benthic solute reservoirs. This is in accordance with the comparatively highest porosity (**Figure 2**) and permeability values of the S-O sediments, which facilitates the exchange with the bottom water in the presence of advective processes. S-S and S-D clustered indistinguishably further right in the

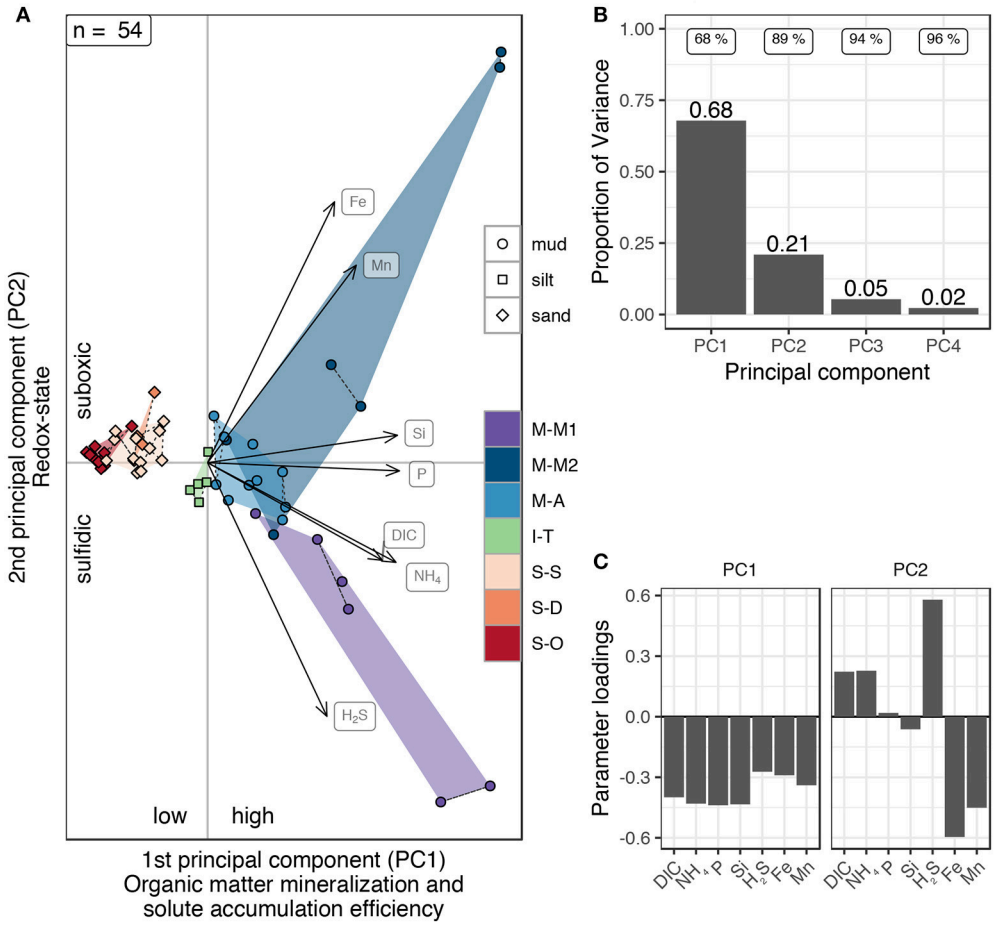

FIGURE 8 | Principal component analysis (PCA) of southern Baltic Sea benthic solute reservoirs in the top 10 cm. **(A)** Each dot represents the mean benthic solute reservoir of *DIC*, NH_4^+, PO_4, H_4SiO_4, sulfide, Fe^{2+}, and Mn^{2+} from parallel cores of each sampling campaign. Shaded areas envelop the expansion of variability of each study site in the two-dimensional space. Dashed lines connect points of the same sampling time. **(B)** Explained variance by different principal components. The first principal component alone explains 68 % and cumulative proportions of the first two principal components explain 89 % of the total variance. **(C)** Loadings of the major two components of the principal component analysis. All considered parameters substantially contribute to PC1. PC2 is loaded with the redox sensitive parameters dissolved sulfide (H_2S), Fe^{2+}, and Mn^{2+} (note the anticorrelation between H_2S and dissolved metals Fe^{2+} and Mn^{2+}) with minor contributions of *DIC* and NH_4^+.

PCA plot (**Figure 8A**), indicating a higher organic matter mineralization and/or solute accumulation potential. Since S-S clearly showed lower oxygen uptake rates (**Figure 3**) and gross sulfate reduction rates (**Figure 5**) compared to S-O sediments, these differences must be attributed to a higher benthic-pelagic solute exchange at the S-O sediment-water interface rather than lower mineralization activity. M-A muds and I-T silts situated in central positions on the x-axis of the PCA plot (**Figure 8A**), suggesting an average organic matter mineralization and/or solute accumulation potential. Although the I-T silt had intermediate TOC contents (**Figure 2**), ChlA contents were significantly higher in I-T than M-A sediments which might indicate higher mineralization rates at this site. Then, the comparatively low reservoirs would suggest a lowered solute accumulation potential than in the studied muds, especially the site M-A. However, since neither the permeability nor the mineralization rates were analyzed at site I-T, it remains unclear whether a different mineralization efficiency or solute accumulation potential of the silty sediment had the larger influence on the difference to the muds.

Further right in the PCA plot, the muddy M-M1 and M-M2 sediments spanned a wide range, indicating great temporal and/or spatial variability. The highest benthic reservoirs were stored in these organic-rich muds, which are impermeable, located in regions with rather calm deposition conditions and therefore less prone to pore water irrigation. M-M1 sediments showed significantly higher pore water sulfide reservoirs in the top 10 cm compared to the other studied muds, which can be partly explained with the comparatively high sulfate reduction rates at this site (**Figure 5**). The differences between the benthic solute reservoirs of the sites M-M1 and the M-M2 were highest and the reservoirs were overall largest during summer (the

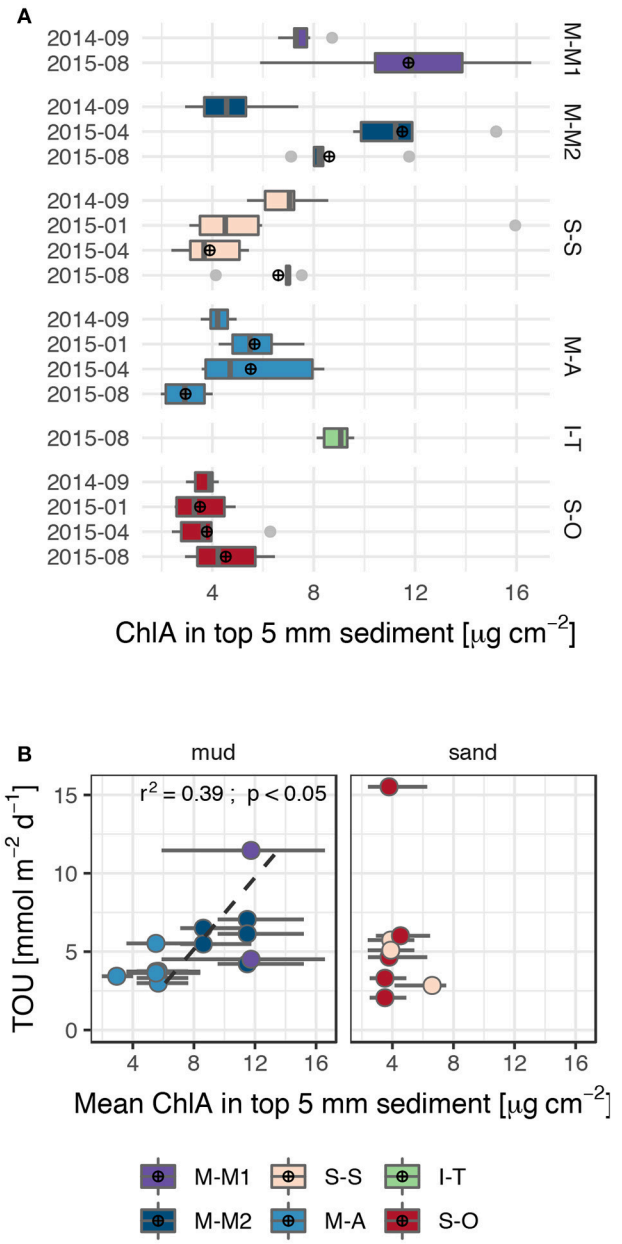

FIGURE 9 | (A) Chlorophyll *a* contents in the top 5 mm surface sediments. Each boxplot summarizes data from multiple sediment cores of one cruise. The left and right hinges of the boxes correspond to the 25 and 75th percentiles, the line within the boxes represents the median. The whiskers extend from the hinges to the largest and smallest value inside the 1.5-fold inter-quartile range. Arithmetic means of the groups used in **(B)** are marked by a ⊕. **(B)** Total oxygen uptake rates vs. mean chlorophyll *a* contents in the top 5 mm of the studied muddy and sandy sediments. Horizontal lines represent the range of values from which the arithmetic mean was calculated.

point pairs furthest to the right in **Figure 8A**). This was likely supported by the higher temperatures during summer in the comparatively shallow stations of the *Bay of Mecklenburg* and can therefore be regarded as seasonal effect.

The second principal component (*PC2*, **Figure 8A**) explained further 21 % of the variance (**Figure 8B**) and was mainly loaded with the redox sensitive parameters sulfide, Fe^{2+} and Mn^{2+} with minor contributions of DIC and NH_4^+ (**Figure 8C**). Negative correlation between sulfide and the reactive metals Fe and Mn was due to the close redox coupling between these elements. The existence of free Fe^{2+} and sulfide in the pore water are mutually exclusive, as the two species precipitate as FeS. Considerable reservoirs of Fe^{2+} and Mn^{2+} can only form by reduction of reactive metal (oxyhydr)oxides where these oxidized phases are frequently or continuously buried by sediment mixing processes, otherwise dissolved sulfide accumulates instead. The variability of near-surface reactive iron contents was likely controlled by particulate inputs from the water column, suggesting an intensive benthic-pelagic Fe turnover. The overall low contents of reactive iron and manganese in the top 10 cm sediments at site M-M1 compared to M-M2 and M-A (**Figure 2**) suggest that this location was decoupled from this cycling for example due to hydrodynamic reasons or hindered bioturbation. Morys et al. (2016) examined the same sites that are covered in this study and found lowest intensities of sediment mixing and also lowest macrozoobenthos abundance and biomass at the M-M1 site. Furthermore, overall highest ChlA contents and SRR values were detected in M-M1 sediments (**Figure 5**) which shifts the suboxic zone closer to the sediment-water interface and narrows it as well. Due to the lack of reaction partners for secondary redox-reactions below the suboxic zone, dissolved sulfide could accumulate in the interstitial waters to high concentrations, while the benthic solute reservoirs in the top 10 cm of the sites M-M2 and M-A were rather controlled by suboxic processes.

Therefore, by the second principal component, mainly the muddy sediments were further classified according to their predominating redox metabolites in the top 10 cm. Highest dissimilarities were evident between summer situations of the adjoining sites M-M1 (sulfidic) and M-M2 (suboxic).

The multi-parameter PCA analysis on the basis of southern Baltic Sea benthic solute reservoirs allowed to clearly differentiate between the studied sites and indicated wide disparities between the different sediment types but also within the studied muds, reflecting fundamental differences in sedimentation conditions, mineralization activity and mixing processes.

4.3. Environmental Control Factors

4.3.1. Bottom Water Salinity Oscillation

The southern Baltic Sea is highly affected by frequent salt water inflows from the North Sea so that the bottom water salinity is usually subject to temporal variability. The *Arkona Basin* is the deepest basin in the southern Baltic Sea study area, deep enough that regular storms do not affect the sediment surface, but shallow enough that seasonal temperature changes reach the bottom waters and also the surface sediments (Leipe et al., 2008). The salinity in the *Arkona Basin* is influenced by the freshwater inflows of the nearby entering *Oder River* as well as by salt water inflows from the North Sea. A stable stratification of the water column in the basin is the consequence of these water sources with different salinity. A major Baltic inflow event occurred at the end of 2014 (Mohrholz et al., 2015) and the resulting

bottom water salinity changes were recorded at the monitoring station *MARNET Arkona* (BSH, 2016). The site M-A, situated close to the *MARNET* monitoring buoy (**Figure 1**), was visited four times during this study between January 2015 and January 2016 after the major Baltic inflow. Bottom water temperature and salinity during these visits ranged from ~5–15 °C and 13–24 respectively, reflecting the variability that is known from the decade-long measurement series at the *Arkona Basin MARNET* station (BSH, 2016). Bottom water salinity variability during this study was clearly higher in the *Arkona Basin* (13–24) than in the *Bay of Mecklenburg* (18–24). These bottom water salinity changes were observed to also affect the pore waters in more than 10 cm depth below the sediment-water interface (e.g., **Figure 6**: Na^+ profiles at site M-A). Pore water concentration profiles of dissolved sodium, representing pore water salinity, quantitatively reflect the influence of bottom water salinity variability on pore water concentration gradients. Considerably higher salinity and thus also higher sulfate concentrations (about 15 mM) were available in the interstitial waters of the top 5 cm during January 2016 compared to September 2015 (about 10 mM sulfate). This implies a strongly enhanced concentration of sulfate, the educt for sulfate reduction, in the top 5 cm of the sediments. Still, gross sulfate reduction rates were higher in the summer situation (**Figure 5**), when bottom water salinity was lowest, compared to the winter situation with much higher bottom water salinity. In addition, generally little variability could be found in the depth gradients of dissolved hydrogen sulfide and the concentrations of organic matter mineralization products (DIC and ammonium) during four visits of the site M-A close to the *MARNET* station (**Figure 6**: site M-A). Despite the serious changes in environmental parameters, the organic matter mineralization derived pore water solutes at site M-A were in a steady-state during this study. Accordingly, we can assume that neither the considerable changes in temperature nor in salinity were the cause for the great spatiotemporal variability in the studied muds of sites M-M1, M-M2, and M-A.

4.3.2. Sediment Mixing

Reactive iron contents considerably above the estimated background levels were detected far below the diffusive oxygen penetration depth of ~1.5–4 mm (**Figure 2**), indicating an active downward transport of oxidized material. The Fe^* profiles often showed a characteristic shape with a maximum close to the sediment water interface, a minimum at ~5–10 cm depth and a second, often broader peak below. Decreasing contents of reactive Fe and Mn with depth (**Figure 2**) indicate active reduction of the oxidized phases, either sulfide-mediated or via microbial dissimilatory metal reduction (Lovley, 1991; Reyes et al., 2017). Released Fe^{2+} and Mn^{2+} migrate up and down along pore water concentration gradients (**Figure 6**) and precipitate as oxides or (oxyhydr)oxides on contact with oxygen near the sediment surface. Precipitation reactions are more likely to occur in the sediment than in the water column, because they are favored by iron and manganese oxide particles and microbially mediated (Thamdrup et al., 1994). Precipitation on contact with hydrogen sulfide from sulfate reduction, either as iron monosulfide (FeS) or pyrite (FeS_2), forms solid phase sulfur reservoirs at depth (**Figure 2**). This characteristic shape, a sharp maximum at the sediment surface, a broader minimum below followed by a second peak at depth, was also found for FeS precipitation in a model study by van de Velde and Meysman (2016), who simulated bioturbation in an idealized coastal muddy sediment. The lower peak was situated at the suboxic-sulfidic interface, where downward diffusing dissolved Fe^{2+} and upward diffusing sulfide meet. Expansion and shrinking of the suboxic zone lead to a vertical shift of the suboxic/sulfidic transition zone so that increased iron sulfide contents are distributed over a broader interval. Manganese is less reactive toward sulfide and therefore remains in solution at depth.

Also profiles of sedimentary mercury (Hg) reflect severe sediment disturbance in the M-M2 sediments (Bunke et al., in review). This type of profile can be found in the sediments of the M-A and S-S site (Bunke et al., 2018, Bunke et al., in review). Going from bottom to top, undisturbed sediments show natural background Hg values at depth ($\leq 50\ \mu g\ kg^{-1}$), a steep increase marking the beginning of the industrialization (about 1900) and a Hg maximum followed by constantly decreasing contents toward the sediment-water interface due to again reduced pollution (Leipe et al., 2013). Also the site M-M1 was characterized by a sharp maximum with highest mercury contents at 18 cm depth. This site is located near a known dumping site of industrial waste material, highly enriched in various contaminants including heavy metals (Kersten et al., 2005; Leipe et al., 2005). However, sediments at the site M-M2 do not show typical Hg gradients, but display instead a thoroughly mixed zone with virtually constant Hg contents in the top ~20–25 cm. Here, the transition from natural background to the anthropogenically affected zone might not mark the beginning of the industrial Hg pollution but the depth down to which sediments were thoroughly mixed, suggesting that these sediments were affected by deep-reaching (25–30 cm) and intensive rearrangement at least once after deposition.

4.3.2.1. Causes of sediment mixing

The site M-A is an aphotic muddy sediment dominated by *Limecola balthica* (Schiele et al., 2015), a surficial modifier penetrating muds and sands up to 5–6 cm deep (Gogina and Zettler, 2010). Morys et al. (2016) found *Limecola balthica*, *Artica islandica*, and *Scoloplos armiger* being the dominant species in M-A muds and responsible for sediment mixing. Advective transport processes across the sediment-water interface include the sediment reworking and water irrigation by the activity of benthic infauna (Aller, 1982; Ziebis et al., 1996; Kristensen et al., 2005) and other processes. Under oxygenated bottom waters, bioturbation, including the transport of both particles and solutes by living organisms either by local (diffusion analog transport) or non-local (directed convective transport) mixing processes, may be the most important sediment mixing process. Layers influenced by bioturbation usually reach 5–10 cm depth, rarely up to 15 cm in surface sediments of coastal marine environments (Aller and Rude, 1988; Aller, 1990, 1994).

However, sediment rearrangement can also be triggered by other processes than bio-mixing. At the site M-M2, Hg profiles indicate intensive sediment rearrangement with mixing depths

of more than 20 cm, which is too deep for most bioturbating infauna. The seabed in this region shows lots of bottom trawl traces, which are clearly recognizable by Side-Scan sonar (Bunke et al., in review). Hopkins (2004) observed imprints in Baltic Sea muddy bottoms of about 0.5–1.0 m depth and 1.0–1.5 m width. It is so far unknown how long these traces last, but significant sediment reworking through bottom trawling must be assumed. Bunke et al., (in review) suggest anthropogenic mixing activity (fishery) as a major sediment rearrangement process in the southern Baltic Sea. Since the bottom trawls mix the sediments only locally, this mixing process may also explain the remarkable redox-dynamics in the M-M2 sediments. In view of the large number of traces and the intensity of the impact on the seabed, anthropogenic mixing via trawl fishery may be the main sediment mixing process at this site.

The site M-A was the by far most constant of all studied sites in this study regarding the sediment pore water signatures in the top 15 cm (**Figure 6**). The study site is located inside the exclusion zone for ship traffic of the *Arkona Basin MARNET* monitoring station (**Figure 1**). It can be assumed that this site is rather unaffected by marine traffic as sidescan sonar recordings in this region revealed essentially no traces of bottom trawl fishing (personal communication Franz Tauber, IOW).

4.3.2.2. Effects of sediment mixing

Significantly higher mineralization rates (TOU and SRR) were measured in the coastal near sites of the *Bay of Mecklenburg* than in the deeper *Arkona Basin*. Increased mineralization activity of the coastal near muds of the *Bay of Mecklenburg* is attributed to enhanced input of fresh organic matter during algal blooms. However, also bioturbation affects early diagenetic processes by modifying the overall reactivity of the sediments (Meysman et al., 2006; Karlson et al., 2007; Kristensen et al., 2012). In sediments underlying oxygenated bottom water, most of organic matter decomposition takes place within the bioturbated zone, and mixing induced redox-oscillation enhances organic matter decomposition compared to constant oxic or anoxic conditions (Aller, 1994). Regular mixing leads to the incorporation of fresh organic matter and oxidants and a continuous removal of inhibitory metabolites which leads to an overall increased degradation of organic material (Aller, 1998). This applies not only to bioturbation but in principle to all sediment mixing processes.

We observed both, downward shifts of the sulfide appearance depth (**Figure 6**) and subsurface reactive iron reservoirs (**Figure 2**) in the sediments of the muddy sites M-M2 and M-A and also at the sandy site S-S. A model study by van de Velde and Meysman (2016) demonstrated the opposing impact of pure particle transport (bio-mixing) and pore water flushing (bio-irrigation) on the development of a suboxic zone in coastal marine sediments. The authors conclude that bio-mixing strongly promotes redox-reactions and cycling of Fe and S, so that stronger and deeper mixing of the top sediment column leads to downward shifts of the sulfide appearance depth and to larger reactive iron reservoirs in the sediment. van de Velde and Meysman (2016) further conclude that bio-irrigation rather removes reduced solutes from the pore water, preventing Fe and S from being recycled within the sediment column and resulting in an overall loss of both solid phase and dissolved Fe and S in irrigated sediments. The sandy site S-O seems to correspond to this pattern as it always showed low sedimentary TS and Fe^* contents (**Figure 2**) and mostly also particularly small pore water concentrations. The site S-O may thus act as a flow reactor with effective transportation of involved reactants, both educts and products, through the surface sediments.

Interestingly, the site M-M1 showed only small subsurface Fe^* contents (**Figure 2**), shallow sulfide appearance depths (**Figure 6**), and overall highest mineralization rates (TOU: **Figure 3** and SRR: **Figure 5**) and benthic solute reservoirs (**Figure 7**). Thus, neither bio-mixing nor bio-irrigation seems to play an important role here although it is near the presumably mixing controlled site M-M2. Particularly low bioturbation potentials were reported for this region, which was attributed to regularly recurring hypoxia and a resulting reduced infauna abundance (Morys et al., 2016).

In the muddy sediments, benthic solute phosphate reservoirs were considerably higher than mineralization of organic matter with the common element ratios of marine organic matter would suggest (subsection 3.4). At comparatively lowest benthic DIC and NH_4^+ reservoirs, the M-M2 station showed the highest phosphate reservoirs of the investigated muds (**Figure 7**). Sedimentary iron oxides control phosphate reservoirs in pore water and solid phase by reversible and irreversible adsorption (Froelich et al., 1982; Sundby et al., 1992; Jensen et al., 1995; Slomp et al., 1996a,b). These reactive iron phases form a barrier against diffusive phosphate transport toward the sediment-water interface, leading to an accumulation of P in the coastal surface sediments (Haese, 2006). As long as the reactive iron phases are not completely reduced or saturated with phosphate, the "iron curtain" efficiently retains phosphate in the sediments. Saturation of the adsorptive surface in the sediments with phosphate is only reached at pore water phosphate concentrations of 10–15 mM (Carman and Wulff, 1989), which is far above the observed concentrations in this study and is thus not likely. Strongly mixed muddy sites like the M-M2 site may thus be an effective sink for P in coastal Baltic Sea sediments.

5. CONCLUSION AND OUTLOOK

Oxygen uptake and sulfate reduction rates were similar in muds and sands, observed variability could essentially be attributed to spatially heterogeneous organic matter inputs. Multi-element pore water concentration gradients in the muds mainly reflected sulfate reduction and consecutive redox-reactions. Suboxic zones of varying extents suggested active downward transport of oxidized material. Coastal basin muds showed most stable geochemical zonation over time, while near-shore bay muds were remarkably dynamic. Orders of magnitude lower pore water concentrations were detected in the sandy sediments, indicating strong and frequent irrigation of the top centimeters, while mineralization products only accumulated below.

The studied sands were, hence, not unreactive substrates but usually rather unable to preserve the mineralization products.

Sands may have a huge importance in coastal marine systems but are underrepresented in most studies and methodologically difficult to investigate. Early diagenetic processes and the impact of intense benthic-pelagic exchange in such shallow marine environments is still poorly understood. Further studies are needed to better understand the driving forces in these environments and their impact on the coastal marine system.

The studied sediments of the southern Baltic Sea showed great dissimilarities with respect to their pore water compositions. Multi-parameter benthic solute reservoirs were shown to reflect early diagenetic processes in surface sediments, including organic matter mineralization, redox-reactions and transport processes. In contrast to diffusive fluxes and transformation rates, parameters usually calculated from pore water profiles, the benthic solute reservoir is an integrated size over a relevant depth range and thus robust against outliers and coarse resolution. In combination with multi-dimensional statistical analysis, namely the principal component analysis (PCA), we were able to clearly differentiate between the studied sites and to identify the processes mainly responsible for the differences between them. The studied sediments differed mainly by (1) their organic matter mineralization and solute accumulation efficiency and (2) their redox-state, reflecting fundamental differences in their sedimentation conditions and mixing processes. The supply of organic matter to the sea floor controlled the overall mineralization activity, while the sediment permeability determined the solute accumulation efficiency of the near-surface sediments.

Strong bottom water salinity variability clearly affected the pore water concentration gradients of the surface sediments but showed no noticeable effects on early diagenetic processes. However, highest dissimilarities were evident between two adjacent sites in a coastal muddy bay. Their varying redox-states could be traced back to different intensities of burial of oxidized material through sediment mixing.

Altogether, advective processes had a particularly strong influence on early diagenetic reactions and benthic solute reservoirs in the top sediments both by irrigation of permeable sands and by rearrangement of cohesive muds. Thus, they are probably the most important cause for spatial and temporal variability of coastal sediments and an important controlling factor for the release/retention of pollutants (e.g., heavy metals) and nutrients (e.g., P) in coastal sediments. In addition to bioturbation, anthropogenic effects can also be considered as potential mixing processes. The influence of sediment rearrangement through bottom trawl fishing on the biogeochemistry of coastal sediments is not sufficiently understood and must be further studied, since a large portion of coastal sediments is regularly affected by trawling equipment.

AUTHOR CONTRIBUTIONS

MB, SF, ML, and JW designed the study. ML performed the sediment and pore water sampling and analysis, the gross sulfate reduction analysis, the benthic solute reservoirs calculations, statistical analysis, and wrote the manuscript. JW and ML conducted core incubation experiments and their evaluation. MG sampled and analyzed benthic macrofauna. JK planned and supervised the gross sulfate reduction analysis at the GFZ. BL developed the reaction-transport models and performed the modeling to evaluate enhanced vertical solute fluxes across the sediment-water interface. CM sampled and analyzed surface sediment ChlA contents. SF performed sediment permeability analysis. All authors contributed to revisions.

FUNDING

This study was supported by German BMBF during the KÜNO projects SECOS-I and -II (03F0666 and 03F0738 A–C), thanks to MB, SF, and Leibniz Institute for Baltic Sea Research. The publication of this article was funded by the Open Access Fund of the Leibniz Association.

ACKNOWLEDGMENTS

We acknowledge the help of Dennis Bunke, Christian Burmeister, Florian Cordes, Andreas Frahm, Michael Glockzin, Axel Kitte, Anne Köhler, Gerhard Lehnert, Tobias Marquardt, Céline Naderipour, Sascha Plewe, Ines Scherff, and Iris Schmiedinger during field sampling and laboratory analysis. The authors wish to thank the captains and crews of R/V Elisabeth Mann Borgese, R/V Poseidon, R/V Alkor, and R/V Maria S. Merian. We wish to thank Boris Chubarenko and Björn Grüneberg for careful reviews that helped to improve the manuscript. Furthermore, Elinor Andrén is thanked for the editorial handling.

SUPPLEMENTARY MATERIAL

The Supplementary Material for this article can be found online at: https://www.frontiersin.org/articles/10.3389/fmars.2018.00413/full#supplementary-material

REFERENCES

Aller, R. C. (1982). "The Effects of Macrobenthos on Chemical Properties of Marine Sediment and Overlying Water," in *Animal-Sediment Relations. Topics in Geobiology,* Vol 100, eds P. L. McCall and M. J. S. Tevesz (Boston, MA: Springer).

Aller, R. C. (1990). Bioturbation and manganese cycling in hemipelagic sediments. *Philos. Trans. R. Soc. Lond. A Math. Phys. Eng. Sci.* 331, 51–68. doi: 10.1098/rsta.1990.0056

Aller, R. C. (1994). Bioturbation and remineralization of sedimentary organic matter : effects of redox oscillationl. *Chem. Geol.* 114, 331–345.

Aller, R. C. (1998). Mobile deltaic and continental shelf muds as suboxic, fluidized bed reactors. *Mar. Chem.* 61, 143–155. doi: 10.1016/S0304-4203(98)00024-3

Aller, R. C., and Rude, P. D. (1988). Complete oxidation of solid phase sulfides by manganese and bacteria in anoxic marine sediments. *Geochim. Cosmochim. Acta* 52, 751–765. doi: 10.1016/0016-7037(88)90335-3

Almroth, E., Tengberg, A., Andersson, J. H., Pakhomova, S. V., and Hall, P. O. J. (2009). Effects of resuspension on benthic fluxes of oxygen, nutrients,

dissolved inorganic carbon, iron and manganese in the Gulf of Finland, Baltic Sea. *Continent. Shelf Res.* 29, 807–818. doi: 10.1016/j.csr.2008.12.011

Al-Raei, A. M., Bosselmann, K., Böttcher, M. E., Hespenheide, B., and Tauber, F. (2009). Seasonal dynamics of microbial sulfate reduction in temperate intertidal surface sediments: controls by temperature and organic matter. *Ocean Dyn.* 59, 351–370. doi: 10.1007/s10236-009-0186-5

Arndt, S., Jørgensen, B. B., LaRowe, D. E., Middelburg, J. J., Pancost, R. D., and Regnier, P. (2013). Quantifying the degradation of organic matter in marine sediments: a review and synthesis. *Earth Sci. Rev.* 123, 53–86. doi: 10.1016/j.earscirev.2013.02.008

Balzer, W. (1984). Organic matter degradation and biogenic element cycling in a nearshore sediment (Kiel Bight). *Limnol. Oceanogr.* 29, 1231–1246. doi: 10.4319/lo.1984.29.6.1231

Berner, R. A. (1980). *Early Diagenesis: A Theoretical Approach*. Princeton, NJ: Princeton University Press.

Bonaglia, S., Deutsch, B., Bartoli, M., Marchant, H. K., and Brüchert, V. (2014). Seasonal oxygen, nitrogen and phosphorus benthic cycling along an impacted Baltic Sea estuary: Regulation and spatial patterns. *Biogeochemistry* 119, 139–160. doi: 10.1007/s10533-014-9953-6

Böttcher, M. E., Hespenheide, B., Llobet-Brossa, E., Beardsley, C., Larsen, O., Schramm, A., et al. (2000). The biogeochemistry, stable isotope geochemistry, and microbial community structure of a temperate intertidal mudflat: an integrated study. *Continent. Shelf Res.* 20, 1749–1769. doi: 10.1016/S0278-4343(00)00046-7

Böttcher, M. E., and Lepland, A. (2000). Biogeochemistry of sulfur in a sediment core from the west-central Baltic Sea: evidence from stable isotopes and pyrite textures. *J. Mar. Syst.* 25, 299–312. doi: 10.1016/S0924-7963(00)00023-3

Boudreau, B. P., Huettel, M., Forster, S., Jahnke, R. A., McLachlan, A., Middelburg, J. J., et al. (2001). Permeable marine sediments: Overturning an old paradigm. *Eos* 82, 133–136. doi: 10.1029/EO082i011p00133-01

Boudreau, B. P., and Westrich, J. T. (1984). The dependence of bacterial sulfate reduction on sulfate concentration in marine sediments. *Geochim. Cosmochim. Acta* 48, 2503–2516. doi: 10.1016/0016-7037(84)90301-6

Bowles, M. W., Mogollón, J. M., Kasten, S., Zabel, M., and Hinrichs, K.-U. (2014). Global rates of marine sulfate reduction and implications for subsea-floor metabolic activities. *Science* 344, 889–891. doi: 10.1126/science.1249213

Brzezinski, M. A. (1985). The si:C:N ratio of marine diatoms: Interspecific variability and the effect of some environmental variables. *J. Phycol.* 21, 347–357. doi: 10.1111/j.0022-3646.1985.00347.x

BSH (2016). *Station Arkona Basin*. Available online at: https://www.bsh.de/DE/DATEN/Meeresumweltmessnetz/_Module/Stationen_mit_Frame/arkona_extern_node.html (Accessed November 18, 2016).

Bunke, D., Leipe, T., and Arz, H. (2018). *Geochemical Depth Profiles of Modern Sediments in the South-Western Baltic Sea*. Available online at: http://iowmeta.io-warnemuende.de/geonetwork/srv/ger/catalog.search#/metadata/IOW-GIS-SECOS-52 (Accessed March 6, 2018).

Burdige, D. J. (2006). *Geochemistry of Marine Sediments*. doi: 10.1086/533614

Canfield, D. E. (1989). Sulfate reduction and oxic respiration in marine sediments: implications for organic carbon preservation in euxinic environments. *Deep Sea Res.* 36, 121–138.

Canfield, D. E., Kristensen, E., and Thamdrup, B. (2005). *Aquatic Geomicrobiology, 1st Edn*. London: Elsevier Academic Press.

Canfield, D. E., Thamdrup, B., and Hansen, J. W. (1993). The anaerobic degradation of organic matter in Danish coastal sediments: iron reduction, manganese reduction, and sulfate reduction. *Geochim. Cosmochim. Acta* 57, 3867–3883. doi: 10.1016/0016-7037(93)90340-3

Carman, R., and Wulff, F. (1989). Adsorption capacity of phosphorus in Baltic Sea sediments. *Estuar. Coast. Shelf Sci.* 29, 447–456. doi: 10.1016/0272-7714(89)90079-6

Cline, J. D. (1969). Spectrophotometric determination of hydrogen sulfide in natural waters. *Limnol. Oceanogr.* 14, 454–458. doi: 10.4319/lo.1969.14.3.0454

Conley, D. J., Stockenberg, A., Carman, R., Johnstone, R. W., Rahm, L., and Wulff, F. (1997). Sediment-water nutrient fluxes in the Gulf of Finland, Baltic Sea. *Estuar. Coast. Shelf Sci.* 45, 591–598. doi: 10.1006/ecss.1997.0246

Dadey, K., Janecek, T., and Klaus, A. (1992). Dry-bulk Density: Its uses and determination. *Proc. Ocean Drill. Program Sci. Results* 126, 551–554.

Eggleton, J., and Thomas, K. V. (2004). A review of factors affecting the release and bioavailability of contaminants during sediment disturbance events. *Environ. Int.* 30, 973–980. doi: 10.1016/j.envint.2004.03.001

Emeis, K. C., Neumann, T., Endler, R., Struck, U., Kunzendorf, H., and Christiansen, C. (1998). Geochemical records of sediments in the Eastern Gotland Basin – products of sediment dynamics in a not-so-stagnant anoxic basin? *Appl. Geochem.* 13, 349–358. doi: 10.1016/S0883-2927(97)00104-2

Field, C. B. (1998). Primary production of the biosphere: integrating terrestrial and oceanic components. *Science* 281, 237–240. doi: 10.1126/science.281.5374.237

Flemming, B. W., and Delafontaine, M. T. (2000). Mass physical properties of muddy intertidal sediments: some applications, misapplications and non-applications. *Continent. Shelf Res.* 20, 1179–1197. doi: 10.1016/S0278-4343(00)00018-2

Fossing, H. (1995). "S-35-radiolabeling to probe biogeochemical cycling of sulfur," in *Geochemical Transformations of Sedimentary Sulfur*, eds. M. A. Vairavamurthy and M. A. A. Schoonen (Washington, DC: American Chemical Society), 348–364.

Froelich, P. N., Bender, M. L., Luedtke, N. A., Heath, G. R., and DeVries, T., (1982). The marine phosphorus cycle. *Am. J. Sci.* 282, 474–511.

Froelich, P. N., Klinkhammer, G. P., Bender, M. L., Luedtke, N. A., Heath, G. R., Cullen, D., et al. (1979). Early oxidation of organic matter in pelagic sediments of the eastern equatorial Atlantic: suboxic diagenesis. *Geochim. Cosmochim. Acta* 43, 1075–1090. doi: 10.1016/0016-7037(79)90095-4

Glud, R. N. (2008). Oxygen dynamics of marine sediments. *Mar. Biol. Res.* 4, 243–289. doi: 10.1080/17451000801888726

Gogina, M., and Zettler, M. L. (2010). Diversity and distribution of benthic macrofauna in the Baltic Sea. Data inventory and its use for species distribution modelling and prediction. *J. Sea Res.* 64, 313–321. doi: 10.1016/j.seares.2010.04.005

Graf, G. (1992). "Benthic-pelagic coupling: a benthic view," in *Oceanography and Marine Biology: An Annual Review,* eds H. Barnes and M. Barnes (Aberdeen: University Press), 149–190.

Grasshoff, K., Kremling, K., and Ehrhardt, M. (2009). *Methods of Seawater Analysis*. Weinheim: John Wiley & Sons.

Haese, R. R. (2006). "The Biogeochemistry of Iron," in *Marine Geochemistry*, eds. H. D. Schulz and M. Zabel (Berlin: Springer-Verlag), 207–240.

Hopkins, C. C. E. (2004). The dangers of bottom trawling in the Baltic Sea. A Report for Coalition Clean Baltic. *Aquat Mar. Advisers.* 1, 1–14. Available online at: https://www.ccb.se/wp-content/uploads/2014/06/bottom_trawling.pdf

Howarth, R. W. (1984). The ecological significance of sulfur in the energy dynamics of salt marsh and coastal marine sediments. *Biogeochemistry* 1, 5–27. doi: 10.1007/BF02181118

Huettel, M., Berg, P., and Kostka, J. E. (2014). Benthic exchange and biogeochemical cycling in permeable sediments. *Annu. Rev. Mar. Sci.* 6, 23–51. doi: 10.1146/annurev-marine-051413-012706

Huettel, M., and Gust, G. (1992). Impact of bioroughness on interfacial solute exchange in permeable sediments. *Mar. Ecol. Prog. Ser.* 89, 253–267. doi: 10.3354/meps089253

Huettel, M., and Rusch, A. (2000). Transport and degradation of phytoplankton in permeable sediment. *Limnol. Oceanogr.* 45, 534–549. doi: 10.4319/lo.2000.45.3.0534

Huettel, M., Ziebis, W., and Forster, S. (1996). Flow-induced uptake of particulate matter in permeable sediments. *Limnol. Oceanogr.* 41, 309–322. doi: 10.4319/lo.1996.41.2.0309

Hyacinthe, C., Anschutz, P., Carbonel, P., Jouanneau, J. M., and Jorissen, F. J. (2001). Early diagenetic processes in the muddy sediments of the bay of biscay. *Mar. Geol.* 177, 111–128. doi: 10.1016/S0025-3227(01)00127-X

Isaksen, M. F., and Jørgensen, B. B. (1996). Adaptation of psychrophilic and psychrotrophic sulfate-reducing bacteria to permanently cold marine environments. *Appl. Environ. Microbiol.* 62, 408–414.

Janssen, F., Faerber, P., Huettel, M., Meyer, V., and Witte, U. (2005). Pore-water advection and solute fluxes in permeable marine sediments (I): Calibration and performance of the novel benthic chamber system Sandy. *Limnol. Oceanogr.* 50, 768–778. doi: 10.4319/lo.2005.50.3.0768

Jensen, H. S., Mortensen, P. B., Andersen, F. O., Rasmussen, E., and Jensen, A. (1995). Phosphorus cycling in a coastal marine sediment, Aarhus Bay, Denmark. *Limnol. Oceanogr.* 40, 908–917. doi: 10.4319/lo.1995.40.5.0908

Jørgensen, B. B. (1977). Distribution of Colorless Sulfur Bacteria a Coastal Marine Sediment. *Mar. Biol.* 28, 19–28.

Jørgensen, B. B. (1978). A comparison of methods for the quantification of bacterial sulfate reduction in coastal marine sediments. *Geomicrobiol. J.* 1, 11–27. doi: 10.1080/01490457809377721

Jørgensen, B. B. (1982). Mineralization of organic matter in the sea bed—the role of sulphate reduction. *Nature* 296, 643–645. doi: 10.1038/296643a0.

Jørgensen, B. B., and Kasten, S. (2006). "Sulfur cycling and methane oxidation," in *Marine Geochemistry*, eds. H. D. Schulz and M. Zabel (Berlin; Heidelberg: Springer), 271–309.

Jørgensen, B. B., and Revsbech, N. P. (1989). Oxygen uptake, bacterial distribution, and carbon-nitrogen-sulfur cycling in sediments from the Baltic Sea-North Sea transition 1937. *Ophelia* 31, 29–49. doi: 10.1080/00785326.1989.10430849

Kallmeyer, J., Ferdelman, T. G., Weber, A., Fossing, H., and Jørgensen, B. B. (2004). A cold chromium distillation procedure for radiolabeled sulfide applied to sulfate reduction measurements. *Limnol. Oceanogr. Methods* 2, 171–180. doi: 10.4319/lom.2004.2.171

Karlson, K., Bonsdorff, E., and Rosenberg, R. (2007). The impact of benthic macrofauna for nutrient fluxes from Baltic Sea sediments. *Ambio* 36, 161–167. doi: 10.1579/0044-7447(2007)36

Kersten, M., Leipe, T., and Tauber, F. (2005). Storm disturbance of sediment contaminants at a hot-spot in the Baltic sea assessed by ²³⁴Th radionuclide tracer profiles. *Environ. Sci. Technol.* 39, 984–990. doi: 10.1021/es049391y

Kostka, J. E., and Luther, G. W. (1994). Partitioning and speciation of solid phase iron in saltmarsh sediments. *Geochim. Cosmochim. Acta* 58, 1701–1710. doi: 10.1016/0016-7037(94)90531-2

Kowalski, N., Dellwig, O., Beck, M., Gräwe, U., Neubert, N., Nägler, T. F., et al. (2013). Pelagic molybdenum concentration anomalies and the impact of sediment resuspension on the molybdenum budget in two tidal systems of the North Sea. *Geochim. Cosmochim. Acta* 119, 198–211. doi: 10.1016/j.gca.2013.05.046

Kristensen, E. (2000). Organic matter diagenesis at the oxic/anoxic interfacein coastal marine sediments, with emphasis on the role of burrowing animals. *Hydrobiologia* 426, 1–24. doi: 10.1023/A:1003980226194

Kristensen, E., Haese, R. R., and Kostka, J. E. (eds) (2005). *Interactions Between Macro-and Microorganisms in Marine Sediments*. Washington, DC: Wiley.

Kristensen, E., Penha-Lopes, G., Delefosse, M., Valdemarsen, T., Quintana, C. O., and Banta, G. T. (2012). What is bioturbation? the need for a precise definition for fauna in aquatic sciences. *Mar. Ecol. Prog. Ser.* 446, 285–302. doi: 10.3354/meps09506

Laima, M. J., Matthiesen, H., Christiansen, C., Lund-Hansen, L. C., and Emeis, K. C. (2001). Dynamics of P, Fe and Mn along a depth gradient in the SW Baltic Sea. *Boreal Environ. Res.* 6, 317–333. Available online at: http://www.borenv.net/BER/pdfs/ber6/ber6-317s.pdf

Laima, M. J., Warszawy, P., and Christiansen, C. (1999). Near-bottom fluxes and composition of suspended matter in the Pomeranian Bay. *Oceanologia* 41, 335–353.

Leipe, T., Harff, J., Meyer, M., Hille, S., Pollehne, F., Schneider, R., et al. (2008). "Sedimentary Records of Environmental Changes and Anthropogenic Impacts during the Past Decades," in *State and Evolution of the Baltic Sea, 1952–2005*, eds. G. Nausch, R. Feistel, and N. Wasmund (Hoboken, NJ: Wiley & Sons).

Leipe, T., Kersten, M., Heise, S., Pohl, C., Witt, G., Liehr, G., et al. (2005). Ecotoxicity assessment of natural attenuation effects at a historical dumping site in the western Baltic Sea. *Mar. Pollut. Bull.* 50, 446–459. doi: 10.1016/j.marpolbul.2004.11.049

Leipe, T., Moros, M., Kotilainen, A., Vallius, H., Kabel, K., Endler, M., et al. (2013). Mercury in Baltic Sea sediments-Natural background and anthropogenic impact. *Chem. Erde Geochem.* 73, 249–259. doi: 10.1016/j.chemer.2013.06.005

Leipe, T., Tauber, F., Vallius, H., Virtasalo, J., Uścinowicz, S., Kowalski, N., et al. (2011). Particulate organic carbon (POC) in surface sediments of the Baltic Sea. *Geo Mar. Lett.* 31, 175–188. doi: 10.1007/s00367-010-0223-x

Llobet-Brossa, E., Rabus, R., Böttcher, M. E., Könneke, M., Finke, N., Schramm, A., et al. (2002). Community structure and activity of sulfate-reducing bacteria in an intertidal surface sediment : a multi-method approach. *Inter Res. Aquat. Microb. Ecol.* 29, 211–226. doi: 10.3354/ame029211

Lovley, D. R. (1991). Dissimilatory Fe (III) and Mn (IV) Reduction. *Microbiol. Rev.* 55, 259–287.

Lovley, D. R., Roden, E. E., Phillips, E. J., and Woodward, J. C. (1993). Enzymatic iron and uranium reduction by sulfate-reducing bacteria. *Mar. Geol.* 113, 41–53. doi: 10.1016/0025-3227(93)90148-O

Mackin, J. E., and Swider, K. T. (1989). Organic matter decomposition pathways and oxygen consumption in coastal marine sediments. *J. Mar. Res.* 47, 681–716.

Meysman, F. J. R., Middelburg, J. J., and Heip, C. H. (2006). Bioturbation: a fresh look at Darwin's last idea. *Trends Ecol. Evol.* 21, 688–695. doi: 10.1016/j.tree.2006.08.002

Middelburg, J. J. (1989). A simple rate model for organic matter decomposition in marine sediments. *Geochim. Cosmochim. Acta* 53, 1577–1581. doi: 10.1016/0016-7037(89)90239-1

Middelburg, J. J., Vlug, T., and Nat, F. J. van der, W. A. (1993). Organic matter mineralization in marine systems. *Global Planet. Change* 8, 47–58.

Moeslund, L., Thamdrup, B., and Jørgensen, B. B. (1994). Sulfur and iron cycling in a coastal sediment: radiotracer studies and seasonal dynamics. *Biogeochemistry* 27, 129–152. doi: 10.1007/BF00002815

Mohrholz, V., Naumann, M., Nausch, G., Krüger, S., and Gräwe, U. (2015). Fresh oxygen for the Baltic Sea – An exceptional saline inflow after a decade of stagnation. *J. Mar. Syst.* 148, 152–166. doi: 10.1016/j.jmarsys.2015.03.005

Morys, C., Forster, S., and Graf, G. (2016). Variability of bioturbation in various sediment types and on different spatial scales in the southwestern Baltic Sea. *Mar. Ecol. Prog. Ser.* 557, 31–49. doi: 10.3354/meps11837

Piker, L., Schmaljohann, R., and Imhoff, J. F. (1998). Dissimilatory sulfate reduction and methane production in Gotland Deep sediments (Baltic Sea) during a transition period from oxic to anoxic bottom water (1993-1996). *Aquat. Microb. Ecol.* 14, 183–193. doi: 10.3354/ame014183

Postma, D., and Appelo, C. A. J. (2000). Reduction of Mn-oxides by ferrous iron in a flow system: Column experiment and reactive transport modeling. *Geochim. Cosmochim. Acta* 64, 1237–1247. doi: 10.1016/S0016-7037(99)00356-7

Poulton, S. W., Krom, M. D., and Raiswell, R. (2004). A revised scheme for the reactivity of iron (oxyhydr)oxide minerals towards dissolved sulfide. *Geochim. Cosmochim. Acta* 68, 3703–3715. doi: 10.1016/j.gca.2004.03.012

R Core Team (2016). *R: A Language and Environment for Statistical Computing*. Available online at: https://www.r-project.org/.

Redfield, A. C. (1958). The biological control of chemical factors in the environment. *Am. Sci.* 46, 230A–221.

Revsbech, N. P., Sorensen, J., Blackburn, T. H., and Lomholt, J. P. (1980). Distribution of oxygen in marine sediments measured with microelectrodes. *Limnol. Oceanogr.* 25, 403–411. doi: 10.4319/lo.1980.25.3.0403

Reyes, C., Dellwig, O., Dähnke, K., Gehre, M., Noriega-Ortega, B. E., Böttcher, M. E., et al. (2016). Bacterial communities potentially involved in iron-cycling in baltic sea and north sea sediments revealed by pyrosequencing. *FEMS Microbiol. Ecol.* 92:fiw054. doi: 10.1093/femsec/fiw054

Reyes, C., Schneider, D., Thürmer, A., Kulkarni, A., Lipka, M., Sztejrenszus, S. Y., et al. (2017). Potentially active iron, sulfur, and sulfate reducing bacteria in skagerrak and bothnian bay sediments. *Geomicrobiol. J.* 34, 840–850. doi: 10.1080/01490451.2017.1281360

Rullkötter, J. (2006). "Organic Matter: The Driving Force for Early Diagenesis," in *Marine Geochemistry*, eds. H. D. Schulz and M. Zabel (Berlin; Heidelberg: Springer), 125–168. doi: 10.1007/3-540-32144-6_4

Rusch, A., and Huettel, M. (2000). Advective particle transport into permeable sediments–evidence from experiments in an intertidal sandflat. *Limnol. Oceanogr.* 45, 523–533. doi: 10.4319/lo.2000.45.3.0525

Rysgaard, S., Fossing, H., and Jensen, M. M. (2001). Organic matter degradation through oxygen respiration, denitrification, and manganese, iron, and sulfate reduction in marine sediments (the Kattegat and the Skagerrak). *Ophelia* 55, 77–91. doi: 10.1080/00785236.2001.10409475

Sawicka, J. E., Jørgensen, B. B., and Brüchert, V. (2012). Temperature characteristics of bacterial sulfate reduction in continental shelf and slope sediments. *Biogeosciences* 9, 3425–3435. doi: 10.5194/bg-9-3425-2012

Schaffer, G., and Collins, H.-J. (1966). "Eine methode zur messung der infiltrationsrate im felde," in *Z. f. Kulturtechnik und Flurbereinigung,* Vol. 7, (Berlin, Hamburg; P. Parey), 193–199.

Schiele, K. S., Darr, A., Zettler, M. L., Friedland, R., Tauber, F., Weber, M. von, et al. (2015). Biotope map of the German Baltic Sea. *Mar. Pollut. Bull.* 96, 127–135. doi: 10.1016/j.marpolbul.2015.05.038

Schippers, A., and Jørgensen, B. B. (2001). Oxidation of pyrite and iron sulfide by manganese dioxide in marine sediments. *Geochim. Cosmochim. Acta* 65, 915–922. doi: 10.1016/S0016-7037(00)00589-5

Schippers, A., and Jørgensen, B. B. (2002). Biogeochemistry of pyrite and iron sulfide oxidation in marine sediments. *Geochim. Cosmochim. Acta* 66, 85–92. doi: 10.1016/S0016-7037(01)00745-1

Seeberg-Elverfeldt, J., Schluter, M., Feseker, T., and Kolling, M. (2005). Rhizon sampling of porewaters near the sediment-water interface of aquatic systems. *Limnol. Oceanogr. Methods* 3, 361–371. doi: 10.1016/S0012-821x(02)01064-6

Skyring, G. W. (1987). Sulfate reduction in coastal ecosystems. *Geomicrobiol. J.* 5, 295–374. doi: 10.1080/01490458709385974

Slomp, C. P., Epping, E. H. G., Helder, W., and Raaphorst, W. V. (1996a). A key role for iron-bound phosphorus in authigenic apatite formation in North Atlantic continental platform sediments. *J. Mar. Res.* 54, 1179–1205. doi: 10.1357/0022240963213745

Slomp, C. P., Van Der Gaast, S. J., and Van Raaphorst, W. (1996b). Phosphorus binding by poorly crystalline iron oxides in North Sea sediments. *Mar. Chem.* 52, 55–73. doi: 10.1016/0304-4203(95)00078-X

Stookey, L. L. (1970). Ferrozine—a new spectrophotometric reagent for iron. *Anal. Chem.* 42, 779–781. doi: 10.1021/ac60289a016

Sundby, B., Gobeil, C., Silverberg, N., and Mucci, A. (1992). The phosphorus cycle in coastal marine sediments. *Limnol. Oceanogr.* 37, 1129–1145. doi: 10.4319/lo.1992.37.6.1129

Talley, L. D., Pickard, G. L., Emery, W. J., and Swift, J. H. (2011). *Descriptive Physical Oceanography: An Introduction.* Amsterdam; Boston: Elsevier-Academic Press.

Tauber, F. (2014). "Regionalized classification of seabed sediments in the German Baltic Sea. BALTIC 2014," in *The 12th Colloquium on Baltic Sea Marine Geology, Warnemünde, September 08-12, 2014,* Abstract Vol. 79. Available online at: www.io-warnemuende.de/conference-bsg2014-schedule.html?file=tl_files/conference/bsg2014/pdf/abstract_volume0809.pdf

Thamdrup, B., Glud, R. N., and Hansen, J. W. (1994). Manganese oxidation and in situ manganese fluxes from a coastal sediment. *Geochim. Cosmochim. Acta* 58, 2563–2570. doi: 10.1016/0016-7037(94)90032-9

Thode-Andersen, S., and Jørgensen, B. B. (1989). Sulfate reduction and the formation of 35S-labeled FeS, FeS2, and S0 in coastal marine sediments. *Limnol. Oceanogr.* 34, 793–806. doi: 10.4319/lo.1989.34.5.0793

van de Velde, S., and Meysman, F. J. R. (2016). The Influence of Bioturbation on Iron and Sulphur Cycling in Marine Sediments: A Model Analysis. *Aquat. Geochem.* 22, 469–504. doi: 10.1007/s10498-016-9301-7

Wang, F., and Chapman, P. M. (1999). Biological implications of sulfide in sediment - A review focusing on sediment toxicity. *Environ. Toxicol. Chem.* 18, 2526–2532. doi: 10.1002/etc.5620181120

Wang, Y., and Van Cappellen, P. (1996). A multicomponent reactive transport model of early diagenesis: application to redox cycling in coastal marine sediments. *Geochim. Cosmochim. Acta* 60, 2993–3014. doi: 10.1016/0016-7037(96)00140-8

Werner, U., Billerbeck, M., Polerecky, L., Franke, U., Huettel, M., Beusekom, J. E. E. van, et al. (2006). Spatial and temporal patterns of mineralization rates and oxygen distribution in a permeable intertidal sand flat (Sylt, Germany). *Limnol. Oceanogr.* 51, 2549–2563. doi: 10.4319/lo.2006.51.6.2549

Winde, V., Böttcher, M. E., Escher, P., Böning, P., Beck, M., Liebezeit, G., et al. (2014). Tidal and spatial variations of DI13C and aquatic chemistry in a temperate tidal basin during winter time. *J. Mar. Syst.* 129, 396–404. doi: 10.1016/j.jmarsys.2013.08.005

Ziebis, W., Huettel, M., and Forster, S. (1996). Impact of biogenic sediment topography on oxygen fluxes in permeable seabeds. *Mar. Ecol. Prog. Ser.* 140, 227–237. doi: 10.3354/meps140227

Conflict of Interest Statement: The authors declare that the research was conducted in the absence of any commercial or financial relationships that could be construed as a potential conflict of interest.